

1 *Review*

## 2 **Surface-modified nanocarriers for nose-to-brain** 3 **delivery: from bioadhesion to targeting**

4 **Fabio Sonvico<sup>1,2,\*</sup>, Adryana Rocha Clementino<sup>1,2</sup>, Francesca Buttini<sup>1,2</sup>, Gaia Colombo<sup>3</sup>,**  
5 **Silvia Pescina<sup>2</sup>, Silvia Stanisçuaski Guterres<sup>4,5</sup>, Adriana Raffin Pohlmann<sup>4,5</sup>, Sara Nicoli<sup>1,2</sup>**

6 <sup>1</sup> Interdipartimental Center for Innovation in Health Products, BIOPHARMANET TEC, University of Parma,  
7 Parco Area delle Scienze 27/a, Parma - 43124, Italy; [e-silvia.pescina@unipr.it](mailto:e-silvia.pescina@unipr.it), [francesca.buttini@unipr.it](mailto:francesca.buttini@unipr.it),  
8 [sara.nicoli@unipr.it](mailto:sara.nicoli@unipr.it)

9 <sup>2</sup> Food and Drug Department, University of Parma, Parco Area delle Scienze 27/a, Parma - 43124, Italy;  
10 [silvia.pescina@unipr.it](mailto:silvia.pescina@unipr.it)

11 <sup>3</sup> Department of Life Sciences and Biotechnology, University of Ferrara, Via Fossato di Mortara 17/19,  
12 Ferrara - 44121, Italy; [clmgai@unife.it](mailto:clmgai@unife.it)

13 <sup>4</sup> Programa de Pós-Graduação em Ciências Farmacêuticas, Universidade Federal do Rio Grande do Sul,  
14 Porto Alegre- 90610-000, Brazil, [silvia.guterres@ufrgs.br](mailto:silvia.guterres@ufrgs.br)

15 <sup>5</sup> Departamento de Química Orgânica, Instituto de Química, Universidade Federal do Rio Grande do Sul,  
16 Porto Alegre - 91501-970, Brazil; [adriana.pohlmann@ufrgs.br](mailto:adriana.pohlmann@ufrgs.br)

17  
18 \* Correspondence: [fabio.sonvico@unipr.it](mailto:fabio.sonvico@unipr.it); Tel.: +39-0521-906282

19

20 **Abstract:** In the field of nasal delivery, one of the most fascinating applications is the delivery of  
21 drugs directly to the central nervous system bypassing the blood brain barrier. This approach would  
22 provide a series of benefits, such as dose lowering and direct targeting of potent drugs, ultimately  
23 reducing their systemic side effects. Recently, clinical trials have explored the nasal administration  
24 of insulin for the treatment of Alzheimer's disease, with promising results. The use of  
25 nanomedicines could provide further options for making nose-to-brain delivery reality. In  
26 particular, apart from the selection of devices able to deposit the formulation in the upper part of  
27 the nose, surface modification of these nanomedicines appears the key strategy to optimize the  
28 delivery of drugs from the nasal cavity to the brain. In this review, nanomedicines delivery  
29 approaches based on surface electrostatic charges, mucoadhesive polymers, as well as chemical  
30 moieties targeting nasal epithelium, will be discussed and critically evaluated for nose-to-brain  
31 delivery.

32 **Keywords:** Nose to brain delivery; Nanoparticles; Pharmaceutical nanotechnology; Mucoadhesion;  
33 Mucus penetrating particles; Targeting; CNS disorders; Neurodegenerative diseases; Alzheimer's  
34 disease; Parkinson's disease.

35

36

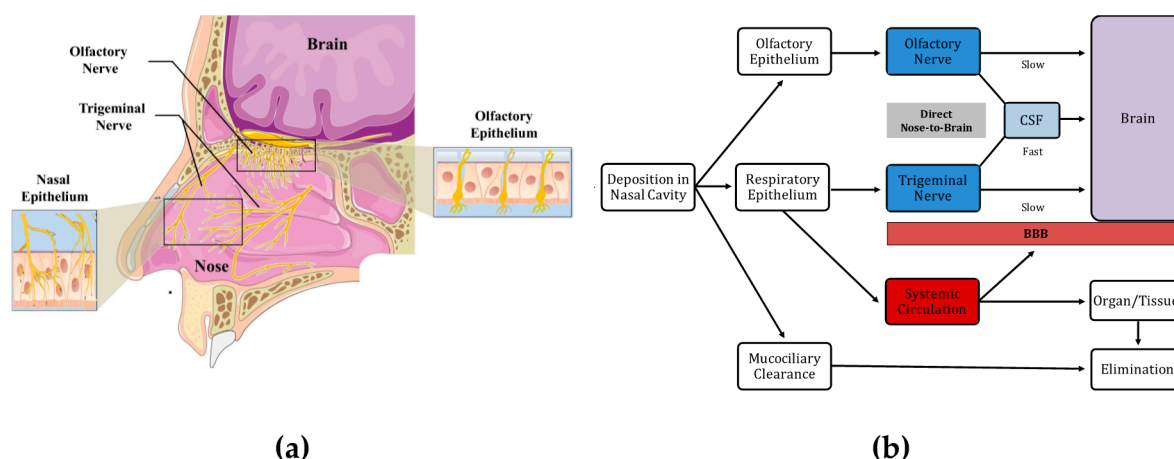
### 37 **1. Pharmaceutical Nanotechnologies for Nose-to-Brain Delivery**

38 Among routes of drug administration that may represent an alternative to the parenteral and  
39 oral ones, nasal delivery has undoubtedly received less attention compared to others, such as the  
40 pulmonary or transdermal delivery routes. Conventionally, nasal drug administration has been  
41 associated to the treatment of minor local ailments such as rhinorrhea, nasal congestion, nasal  
42 infections and allergic or chronic rhinosinusitis [1]. However, nasal delivery shows a high number of  
43 clear advantages, such as ease of administration, non-invasiveness, good patient compliance, rapid  
44 onset of action, relatively large and permeable absorption surface, reduced enzymatic activity and  
45 avoidance of hepatic first-pass metabolism. Therefore, an increasing number of products exploiting

46 the nose as site of administration for the systemic delivery of small and large molecules (including  
47 peptides, proteins and vaccines) are being developed and are reaching the market. In this context,  
48 nasal delivery is one of the most versatile routes of administration with applications going from  
49 smoke cessation (nicotine, Nicotrol® NS, Pfizer, USA) to flu vaccination (live attenuated influenza  
50 vaccine, FluMist® Quadrivalent, Astra Zeneca, USA), from pain management (fentanyl, Instanyl®,  
51 Takeda, Japan and Pecfent/Lazanda®, Archimedes Pharma Ltd., UK; butorphanol tartrate spray,  
52 Mylan Inc., USA) to postmenopausal osteoporosis (salmon calcitonin, Fortical®, Upsher-Smith, USA),  
53 from the treatment of migraine (zolmitriptan, Zomig®, AstraZeneca, UK; sumatriptan, Imigran, GSK,  
54 UK and Onzetra™ Xsail™, Avanir Pharmaceuticals, USA) to that of endometriosis (nafarelin,  
55 Synarel®, Pfizer, USA) or prostate cancer (buserelin, Suprecur®, Sanofi-Aventis, France) [2].  
56

57 Seemingly, however, the best is yet to come, as the nasal cavity offers a unique opportunity for  
58 the delivery of pharmaceutically active ingredients (APIs) to the central nervous system (CNS).  
59 Considering the increasing incidence of brain diseases and neurological disorders associated with the  
60 aging population, achieving efficient drug delivery to the brain is one of the priorities of modern  
61 pharmaceutical sciences. However, brain delivery of drugs is a complex challenge, as the CNS is  
62 protected by the blood brain barrier (BBB) and blood cerebrospinal fluid barrier (BCSFB), two  
63 formidable structures providing a selective brain permeability to circulating molecules. These  
64 physical, metabolic and transporter-regulated barriers tremendously limit the number of  
65 pharmacologically active substances able to access the CNS at therapeutic concentrations [3]. Several  
66 approaches have been proposed to improve brain delivery across BBB [3,4], including  
67 nanoparticulate drug carriers targeting specific transporters present on the BBB [5-7]. Unfortunately,  
68 the percentage of injected drug dose reaching the brain even with BBB targeting or permeation  
69 enhancing strategies is below 5%, typically less than 1%, with the remaining 95-99% of the drug off-  
70 target and potentially responsible for systemic side effects. Furthermore, in the case of nanocarriers,  
71 the CNS chronic toxicity and immunogenicity of polymers, surfactants and other components must  
72 be carefully evaluated, especially considering the prolonged treatments required for CNS diseases  
73 [8].  
74

75 An increasing number of studies suggests that intranasal drug delivery enables brain delivery  
76 of both small and large molecules actually bypassing the BBB via the nerves present in the nasal  
77 cavity, *i.e.* the olfactory and trigeminal nerves. In particular the olfactory 'neuroepithelium', present  
78 exclusively in the nasal cavity, is the only part of the CNS that is in direct contact with the external  
79 environment. Consequently, it is a unique access port to the brain [9]. On the other hand the  
80 trigeminal nerve has been demonstrated to be significantly involved in the nose-to-brain (N2B)  
81 delivery of certain substances, especially towards the posterior region of the brain [10,11]. As a  
82 consequence, drugs can reach the CNS following nasal administration via three main pathways,  
83 namely: A) the olfactory nerve pathway, which innervates the olfactory epithelium of the nasal  
84 mucosa and terminates in the olfactory bulb, B) the trigeminal nerve pathway, which innervates,  
85 through its ophthalmic and maxillary branches, both the respiratory and (to a lesser degree) the  
86 olfactory epithelium and terminates in the brainstem and olfactory bulb, respectively, and C) the  
87 vascular pathway. Among these, the olfactory and trigeminal nerve pathways provide brain delivery  
88 either via a slow intracellular axonal transport (hours or even days) or fast perineural paracellular  
89 transport (minutes) from the sub-mucosal space to the cerebrospinal fluid (CSF) compartment [12,13].  
90 The vascular pathway provides a secondary, indirect mechanism of delivery, whereby the drug is  
91 firstly absorbed into systemic circulation and subsequently transported to the brain across the BBB  
92 [14]. Figure 1 outlines the nasal innervation and the three brain-targeting pathways of nasal delivery.  
93



94

95

96

**Figure 1.** (a) Nasal innervation; (b) Nose-to-brain (N2B) pathways of drug delivery (modified from [15] and [16]).

97 Hence, nasal delivery has been proposed for the treatment of various central nervous system  
 98 conditions, such as migraine [17], sleep disorders [18], viral infections [19], brain tumors [20,21],  
 99 multiple sclerosis (MS) [22], schizophrenia [23], Parkinson's disease (PD) [24], Alzheimer's disease  
 100 (AD) [25] and even for the treatment of obesity [26]. However, several limitations can be envisaged  
 101 such as small nasal cavity volume, limited amount of formulation that can be administered, poor  
 102 olfactory region deposition from conventional nasal devices, short mucosal contact time due to the  
 103 mucociliary clearance, poor bioavailability of hydrophilic and/or large molecules, mucosal irritation  
 104 and lack of validated translational animal models [27]. All these may negatively affect the potential  
 105 of the nose-to-brain transport, to the point that some authors around the mid 2000's doubted whether  
 106 such approach could be exploited therapeutically in humans [28,29].

107 Since then, a number of nasal devices specifically able to deposit nasal formulation in the  
 108 olfactory region of the nasal cavity, such as ViaNase atomizer (Kurve Technologies, USA),  
 109 pressurized Precision Olfactory Device (Impel Neuropharma, USA) and the liquid and powder  
 110 Exhalation Delivery Systems (OptiNose, USA), have been designed and are now available for the  
 111 development of new medicinal products [30].

112 Preclinical studies in animals increasingly use specific indexes to quantify the efficiency of brain  
 113 delivery following administration, such as nose-to-brain drug targeting efficiency (DTE, Equation 1)  
 114 and direct transport percentage (DTP, Equation 2) [31]. Drug targeting efficiency index provides the  
 115 exposure of the brain to the drug after nasal administration relative to that obtained by systemic  
 116 administration:

117

$$DTE = \frac{\left( \frac{AUC_{Brain}}{AUC_{Blood}} \right)_{IN}}{\left( \frac{AUC_{Brain}}{AUC_{Blood}} \right)_{IV}} \cdot 100, \quad (1)$$

118

119 where  $AUC_{Brain}$  and  $AUC_{Blood}$  are the area under the concentration *vs.* time curves of the drug in the  
 120 brain and in the circulation (blood, plasma or serum) after intranasal (IN) and intravenous (IV)  
 121 administration. DTE values can range from 0 to  $+\infty$ , with values above 100% representing a more  
 122 efficient brain targeting after IN administration *vs.* IV, whereas values below 100% indicate the  
 123 opposite.

124 Direct transport percentage index calculates the estimated fraction of the dose reaching the brain via  
 125 direct nose-to-brain pathways over the cumulative amount of drug reaching the brain after intranasal  
 126 delivery:

127

$$DTP = \frac{B_{IN} - B_x}{B_{IN}} \cdot 100, \quad (2)$$

128

129 where  $B_{IN}$  is the brain AUC following intranasal administration, and  $B_x$  is the fraction of the same  
130 AUC due to the drug crossing the BBB from systemic circulation calculated according to Equation 3:

131

$$B_x = \frac{B_{IV}}{P_{IV}} \cdot P_{IN}, \quad (3)$$

132

133 where  $P_{IN}$  and  $P_{IV}$  are the blood AUC after intranasal and intravenous administration, respectively.  
134 DTP positive values up to 100 indicate a contribution of the direct nose-to-brain pathways to brain  
135 drug levels, whereas DTP equal to 0 (or even negative) indicates a preferential brain accumulation  
136 after IV administration of the drug. This quantitative preclinical pharmacokinetics data associated  
137 with pharmacodynamics results allows for the creation of advanced translational PK and PK-PD  
138 models able to predict CNS concentrations in humans [32].

139

140 Furthermore, some clinical trials on brain delivery in humans of nasally delivered drugs, such  
141 as insulin for the treatment of Alzheimer's disease [33,34], oxytocin for autism [35], schizophrenia  
142 and major depressive disorder [36] and davunetide for mild cognitive impairment [37,38] and  
143 progressive supranuclear palsy [39], clearly demonstrate that the N2B delivery has been considered  
144 since 2012 a viable and promising clinical approach by several pharmaceutical companies [40].

145

146 Despite all these advancements, the delivery of drugs presenting unfavorable physico-chemical  
147 and biopharmaceutical characteristics such as rapid chemical or enzymatic degradation, poor  
148 solubility, low permeability and low potency requires a formulation able to promote the mechanisms  
149 of transport of the drug to the brain, without disrupting the structure and physiologic function of the  
150 nasal epithelium.

151 Pharmaceutical nanotechnologies appear as an ideal formulative strategy for the N2B delivery  
152 of these "problematic" substances, including peptide and proteins. In fact, nano-sized (1-1000 nm)  
153 drug delivery systems can:

154

- 154 • Protect the encapsulated drug from biological and/or chemical degradation;
- 155 • Increase apparent drug water-solubility;
- 156 • Enhance residence time at the site of absorption;
- 157 • Promote mucosal permeation and/or cellular internalization;
- 158 • Control the release kinetics of the encapsulated drug;
- 159 • Achieve targeted drug delivery through surface modification with specific ligands;
- 160 • Reduce drug distribution to non-target sites, minimizing systemic side effects.

161

162 All these features appear desirable for an efficient N2B delivery and are potentially critical to enable  
163 the therapeutic application of drugs that without a proper carrier would not reach the CNS at  
164 sufficient concentrations to elicit a pharmacological response.

165 Therefore, almost all types of pharmaceutical nanocarriers have been studied for nose-to-brain  
166 delivery, including and not limited to nanocrystals [41,42], micelles [43,44], liposomes [45], solid lipid  
167 nanoparticles (SLN) [46,47], nanostructured lipid carriers (NLC) [48,49], polymeric nanoparticles [50-  
168 52], albumin nanoparticles [53], gelatin nanoparticles [53], dendrimers [54], mesoporous silica  
169 nanoparticles [55], nanoemulsions [56].

170

171 In consequence of such an intense research activity in this field, several reviews have been  
172 published recently on the use of nanoparticles for the N2B delivery, covering both general [57-61]  
173 and specific disease [62,63] or vector-related topics [64-66]. Hence, the present review does not aim  
174 to provide an exhaustive report on the various applications of nanoparticles administered nasally

175 allowing for a direct drug delivery to the brain. In contrast, it collects and appraises critically some  
176 facts and figures related to the leading strategies of nanoparticle design for nose-to-brain delivery. In  
177 particular, the review will focus on nanoparticles physico-chemical characteristics and surface  
178 modification with mucoadhesive, penetration enhancing or targeting moieties, able to affect and  
179 promote the brain delivery of therapeutically active substances.  
180

## 181 2. Influence of Physico-chemical Properties in Nanoparticles Nose-to-Brain Delivery

182 Many papers have described enhanced delivery to the brain after nasal administration of  
183 nanoencapsulated drugs in comparison with simple drug solutions. However, few studies draw  
184 attention on the precise mechanism through which nanoparticles enhance drug transport to the brain.  
185 Different scenarios can be depicted, from the simplest one, where the nanocarriers just interact with  
186 the mucus layer and release the drug in the mucus or at the mucus/epithelial cell interface, to the  
187 most “challenging” that see the drug-loaded nanoparticles crossing the mucosal barrier, being  
188 uptaken by neurons and translocated along the axons of trigeminal and olfactory nerves to reach the  
189 brain, where the drug is released. In the middle, there is the possibility of nanoparticle uptake into  
190 the respiratory epithelium and/or through olfactory neuroepithelium, where the payload is released  
191 and then the drug diffuses along perineural spaces to reach the CNS. It is clear that the fate of particles  
192 depends on the physicochemical characteristics of the nanoparticles themselves. Indeed,  
193 composition, size, surface charge, shape and surface hydrophobicity/hydrophilicity have an impact  
194 on nanocarrier interaction with the biological environment. In the case of nose-to-brain delivery,  
195 these features influence the interaction with the mucus, the uptake in the epithelial and  
196 neuroepithelial cells, the translocation to the brain by diffusion along the axons and the release  
197 kinetics of the drug. In this context, the elucidation of the role of physicochemical properties of NP is  
198 essential to be able to design both efficient and safe carriers.  
199

200 In order to clarify the role of NP characteristics such as particle size, surface charge,  
201 hydrophobicity on their fate, some authors have studied nanoparticles transport either *in vitro* across  
202 olfactory cells monolayer, *ex vivo* across excised nasal mucosa, or *in vivo* on rat /mouse models.

203 In a recent paper Gartzandia *et al.* [67] have compared the permeability of nanoparticles having  
204 different physico-chemical properties across rat olfactory mucosa primary cells monolayers. A  
205 fluorescent probe (DiR; 1-1'-dioctadecyl-3,3',3' tetranethylindotricarbocyanine) was loaded to track  
206 the particles: previous studies demonstrated the absence of probe release in the transport buffer. The  
207 authors found significant differences in nanoparticle permeation as a function of the constituting  
208 material: nanostructured lipid carriers (NLC) penetrated to a higher extent compared to PLGA  
209 nanoparticles having the same zeta potential (-23 mV). The change of the surface potential of NLC  
210 from negative to positive by chitosan coating determined an almost 3 folds increase in the  
211 transcellular transport compared to the uncoated NLC. Finally, the surface functionalization using  
212 cell-penetrating peptides (in particular Tat) further enhanced nanoparticle transport. While the role  
213 of chitosan can be explained considering an electrostatic interaction with the negatively charged cells,  
214 the different performance observed deserves further investigation before attributing it to  
215 nanoparticle constituents, *i.e.* polymeric *vs.* lipid particles. Indeed, the particles analyzed had  
216 different size (*approx.* 100 nm for NLC and 220 nm for PLGA nanoparticles) and different surfactants  
217 were used for their preparation: while NLC were made using polysorbate 80 and poloxamer (*i.e.* PEG  
218 moieties could be found on NP surface), PVA was used as surfactant for PLGA nanoparticles. This  
219 can contribute to the differences found considering the mucus-penetrating properties of PEG (see  
220 also section 4.1) and the mucoadhesive properties of PVA-coated particles, reported to interact with  
221 mucus constituents by hydrogen bonding and/or hydrophobic interactions [68].

222 Musumeci and collaborators [69] prepared PLGA, PLA and chitosan nanoparticles using  
223 polysorbate 80 (Tween 80) as surfactant and rhodamine as fluorescent probe. They found a higher  
224 uptake in olfactory ensheathing cells (extracted from rat pups olfactory bulbs) for PLGA NP (132 nm,  
225 -15.8 mV) compared to chitosan (no surfactant, 181 nm, +34 mV) and PLA (152 nm, -30 mV)

226 nanoparticles. In this case, the higher uptake of PLGA nanoparticles compared to the others was  
227 explained by the authors considering the lower absolute superficial charge, but the presence of PEG  
228 moieties on PLGA and PLA particle surface could have also contributed to the obtained result.  
229 However, it is difficult to compare the data from the two previously cited studies since different cells  
230 were used. It is known that the type and the physiological status of the cell highly influence its  
231 behavior toward nanoparticle uptake [70].

232 Mistry *et al.* [71] adopted a more complex barrier, *i.e.* excised porcine olfactory epithelium  
233 mounted on Franz-type diffusion cells, to compare the behavior of carboxylate-modified fluorescent  
234 polystyrene nanoparticles measuring 20, 100 and 200 nm in size ( $\zeta$  potential: approx. -42 mV) with  
235 surface-modified nanoparticles obtained by coating with chitosan (48, 163 or 276 nm;  $\zeta$  potential  
236 approx. +30 mV) or polysorbate 80 ( $\zeta$  potential approx. -21 mV). None of the tested particles crossed  
237 the nasal epithelium after 90 minutes, but polysorbate 80-coated (PEGylated) particles penetrated  
238 deeper in the tissue compared to uncoated and chitosan-coated nanoparticles. On the other hand, the  
239 number of particles present at the epithelial surface was higher in case of chitosan coated particles,  
240 and histological images suggested a localization within the mucus layer. No clear trend was found  
241 concerning the influence of nanoparticle size on drug uptake into the tissue.

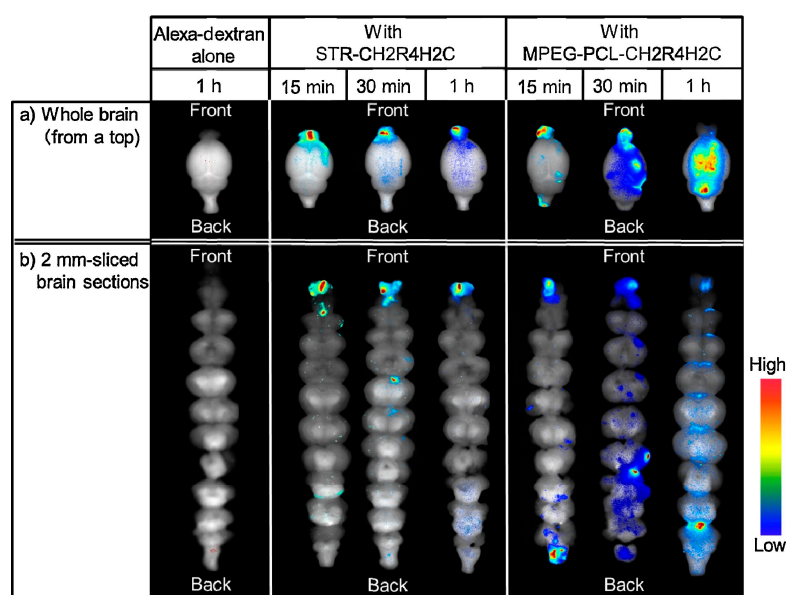
242 The same nanoparticles were also evaluated *in vivo* on a mice model [72]. 15  $\mu$ l of formulation  
243 containing either 105 nm polystyrene nanoparticles (-42 V), 163 and 276 nm chitosan-coated NP ( $\zeta$   
244 potential +30 and +23 mV respectively) or 107 and 180 nm polysorbate 80 coated NP ( $\zeta$  potential -21  
245 and -24 mV respectively) were applied daily for 3 days. All nanoparticles were transported to some  
246 extent across the mucosa (both olfactory and respiratory) via a transcellular route. The presence of  
247 polysorbate 80 coating did not enhance tissue uptake as compared to the uncoated particles, despite  
248 the claimed mucus penetrating properties of PEG. The authors explained these results considering  
249 that the PEG chains were not covalently bound to the particles, and that a precise length and density  
250 of PEG chains is needed to obtain a relevant mucus penetrating effect [73,74]. A significant difference  
251 was found between 107 and 180 nm polysorbate 80 coated NP ( $\zeta$  potential -21 and -24 mV  
252 respectively), and the lower accumulated amount measured for the bigger particles was attributed to  
253 a slower diffusion inside the mucus network. Chitosan-coated particles were mainly retained inside  
254 the mucus and lower amounts were found in the tissue in comparison with uncoated and polysorbate  
255 80-coated nanoparticles. Despite the long application time (4 days) nanoparticles were never found  
256 in the olfactory bulb, regardless the size or the superficial properties.

257 Ahmad [75] studied the permanence of a nanoemulsion made with  
258 Labrafac®WL1349/Labrafac®CC and Solutol®HS15 in the nasal cavity of rats from 0.5 to 16 hours after  
259 the application of 100  $\mu$ l of formulation. In particular, nanoemulsions with droplets of 80, 200, 500  
260 and 900 nm (NE80, NE200, NE500 and NE 900) were compared. The droplets were tracked with  
261 environment-responsive probes giving a fluorescent signal when dispersed in the nanocarrier matrix  
262 that is quenched immediately after release. It was found that the smaller the droplet size, the higher  
263 the retention in the nasal cavity. The even longer retention obtained with positively charged chitosan-  
264 coated nanodroplets (size 108 nm) was attributed to the electrostatic interaction with the mucus and  
265 with the negatively charged epithelial membranes. Further evaluations were done with NE80, NE900  
266 uncoated nanoemulsions and the chitosan-coated nanoemulsion 108 nm in size. After 1 h from the  
267 nasal instillation a large number of nanoemulsion droplets were present in the nasal mucosa, the  
268 highest signal was found for the chitosan-coated nanoemulsion, followed by NE80 and NE900  
269 uncoated nanoemulsions. In the trigeminal nerve the translocation was size-dependent being ranked  
270 NE80 > Chitosan coated > NE900. Accumulation in the brain (and in particular in the olfactory bulb)  
271 was also assessed: only minimal numbers of NE droplets entered the brain after 1 h, and these were  
272 only visualized in case of particles with small size (NE80 and 108 nm, chitosan coated), in agreement  
273 with the *in vivo* results obtained by Mistry [72].

274 Differently, a recent paper reported significant brain accumulation of PLGA nanoparticles after  
275 nasal administration in rats. The authors prepared rhodamine-loaded PLGA nanoparticles  
276 (surfactant: polysorbate 80, size 118 nm,  $\zeta$  potential -26 mV) and chitosan-PLGA nanoparticles  
277 (213nm, +69 mV) and analyzed the brain distribution of fluorescence after 8, 24 or 48 h from the

278 intranasal administration. The results evidenced that both positively and negatively charged particles  
 279 could reach the brain and were localized mainly in the cytosol of the neural cells. Different  
 280 localization (caudal *vs.* rostral area) could be obtained by modifying the surface charge. A particle  
 281 distribution as a function of the post-application time was also described, with slower brain uptake  
 282 for positively charged particles, attributed to both mucus-nanoparticle interaction in the nasal cavity  
 283 and a different nose-to-brain pathway. The authors hypothesized that the slower translocation of  
 284 positive particles was due to an intra-neuronal pathway (trigeminal nerve), whereas the extra-  
 285 neuronal pathway, relying on bulk flow transport, was responsible for the rapid transport of  
 286 negatively charged particles. Despite the interesting results, no experimental evidence, with the  
 287 exception of the different timing of brain appearance, supported the hypothesis and the involvement  
 288 of different (systemic) pathways could not be excluded.

289 A specific brain distribution as a function of the properties of the nanocarriers was also described  
 290 by Kanazawa *et al.* [76] by using peptide-based carriers. An arginine-rich oligopeptide (designed to  
 291 have adhesiveness and transmissibility) was conjugated with either a hydrophobic moiety (stearic  
 292 acid) or a hydrophilic one (PEG-PCL block copolymer) in order to obtain two stable micellar  
 293 formulations. An Alexa-dextran complex (MW 10,000 Da) was used as fluorescent probe to assess  
 294 biodistribution. The stearate-peptide and PEG-PCL-peptide micelles were 100 and 50 nm in size and  
 295 had a  $\zeta$  potential of +20 and +15 mV, respectively. After intranasal application in rats, the two carriers  
 296 determined a much higher uptake in the nasal mucosa and in the brain as compared to Alexa-dextran  
 297 alone. The hydrophobic stearate-peptide determined a markedly higher fluorescence in the nasal  
 298 epithelium compared to the hydrophilic PEG-PCL-peptide, but a lower fluorescence in the trigeminal  
 299 nerve. Additionally, when analyzing the intracerebral distribution pattern of Alexa (Figure 2) as a  
 300 function of the time post-intranasal administration, a significant difference between the two carriers  
 301 could be appreciated: hydrophobic stearate-peptide showed a strong fluorescence in the forebrain  
 302 after 15 minutes, 30 minutes and 1 hour and no transport to the hindbrain was evidenced. In contrast,  
 303 upon PEG-PCL-peptide administration, a spreading of the fluorescence after 30 minutes and 1 hour  
 304 was evident, indicating a distribution of Alexa to the entire brain. This result, together with the higher  
 305 trigeminal fluorescence, suggests that PEG-PCL-peptide nanocarriers penetrated across the nasal  
 306 mucosa and transported the probe to both the olfactory bulb (forebrain) and to the hindbrain via the  
 307 olfactory and trigeminal nerves.  
 308



309

310 **Figure 2.** Dynamics of Alexa-dextran in brain tissue following NASAL administration of hydrophobic  
 311 (STR-CH2R4H2C) and hydrophilic (MPEG-PCL CH2R4H2C) surface nanocarriers in: (a) Whole brain  
 312 and (b) 2 mm-sliced brain sections (reprinted with permission from [76]).

313

314 Gabal *et al.* [77] evaluated the impact on N2B delivery of the nanoparticle surface charge by  
315 preparing anionic and cationic NLC having very similar size (175 nm and 160 nm respectively) and  
316 opposite  $\zeta$  potential values (-34 and +34 mV respectively), encapsulating the same amount of drug  
317 (ropinirole HCl, EE% 53 and 50%, respectively) and characterized by a very similar release kinetics  
318 *in vitro*. These nanoparticles were dispersed in a thermosensitive gel made of poloxamers (407 and  
319 188) and HPMC and administered intranasally in albino rats. Animals were sacrificed 3 to 360  
320 minutes after the intranasal application and drug levels were measured in plasma and brain to  
321 calculate the pharmacokinetic parameters. Overall, there was no significant difference between  
322 negative and positive nanoparticles and both performed much better than a drug solution. However,  
323 the actual contribution of the nanocarrier is not clear since the improved bioavailability appears  
324 mainly due to the increased residence time given by the gel and/or to the presence of a penetration  
325 enhancer (sodium deoxycolate) in the nanoparticle formulation. Indeed, the authors also compared  
326 the toxicity of anionic NLC, cationic NLC and the nanocarriers dispersed in the gel after 10  $\mu$ l  
327 application daily for 14 days in rats. The results highlighted the highest toxicity for cationic NLC, a  
328 lower toxicity for anionic NLC while no histopathological alterations were found in animals treated  
329 with gels loaded either with cationic or with anionic particles. The authors attributed this finding to  
330 a direct protective mechanism of poloxamer 188 against oxidative stress and inflammation. However,  
331 the hindered nanoparticle diffusion through the gel network and the consequent limited interaction  
332 between nanoparticles and epithelium may be considered the real reasons of the reduced toxicity  
333 evidenced.

334

335 The potential toxicity of nanoparticles on the mucosa and also to CNS structures is a critical  
336 point, related to the physicochemical properties, to be taken into account in nose-to-brain  
337 applications. In agreement with the above-mentioned results, also other authors described a higher  
338 toxicity of positively charged nanoparticles: chitosan-coated nanoparticles applied in a pH 6.0 citrate  
339 buffer vehicle had a size-dependent damaging effect on the excised porcine olfactory epithelium: 20  
340 nm nanoparticles caused substantial tissue damage as compared to 100 and 200 nm nanoparticles  
341 [71]. This effect can be partially attributed to the buffer, but also to the high relative surface area,  
342 combined with the presence of the positive surface charge. However, it is worth mentioning that  
343 toxicity studies on animal models have evidenced a substantial safety of nanoparticles made or  
344 coated with chitosan [78] suggesting that *in vivo* the presence of a thicker mucus can reduce the toxic  
345 effect, probably by reducing the interaction between nanoparticles and epithelium.

346 Extensive nanotoxicological literature showed the capability of pollutants and metal  
347 nanoparticles to reach the brain parenchyma after nasal instillation or inhalation and, in some cases,  
348 to elicit toxic effect on the CNS [79-81]. A careful selection of the excipients used is thus mandatory  
349 and rapid and efficient biodegradation within the absorption tissue appears the best strategy to avoid  
350 unwanted accumulation and potential CNS toxicity of the innovative nanocarrier.

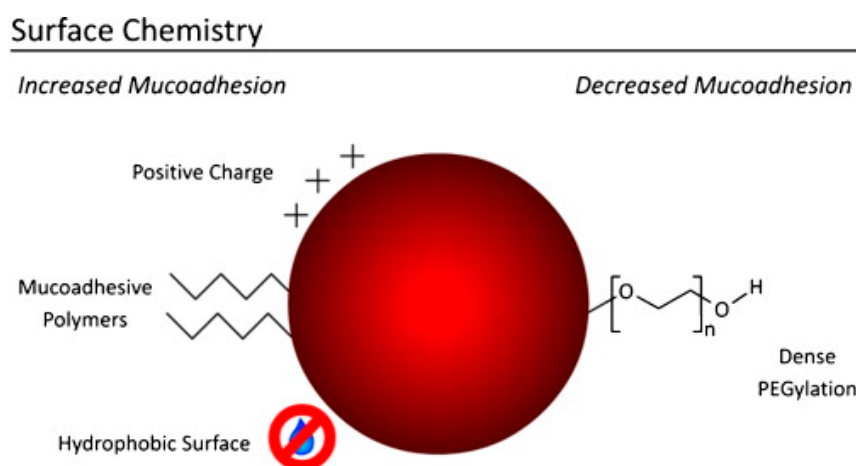
351

### 352 3. Mucoadhesive Nanoparticles

353 One of the physiological factors having a significant impact on nasal delivery and on N2B  
354 transport is mucociliary clearance. This physiological protection mechanism of the respiratory system  
355 allows for an efficient and rapid elimination of noxious substances, particulate matter and  
356 microorganisms trapped in the mucus layer (10-15  $\mu$ m thick) during air intake (clearance  $t_{1/2}$  20  
357 minutes in humans). However, this appreciably limits the residence time of substances administered  
358 inside the nasal cavity. As a consequence, traditional nasal formulations exploited excipients able to  
359 increase viscosity and/or provide bioadhesion, such as hydrophilic polymers, to reduce mucociliary  
360 clearance, prolong formulation residence time, improve systemic bioavailability and reduce nasal  
361 absorption variability [82]. The mucus lining the nasal epithelium is secreted by goblet cells present  
362 in the epithelium itself and mainly by submucosal glands present in the lamina propria. It is  
363 composed of about 90-95% water, 2-5% mucins, 1% salts and variable amounts of cellular products  
364 and debris such as DNA, albumin, immunoglobulins, lysozyme, lactoferrin, and lipids [73,83]. In

365 particular, the highly glycosylated proteins mucins (10-40 MDa) are the major determinant of mucus  
 366 properties. These glycoproteins, because of their molecular weight, hydration, crosslinking and  
 367 entanglement, confer to the nasal secretion viscosity and elasticity, typical of a non-Newtonian  
 368 thixotropic gel. In addition, mucins present a high sialic acid and sulfate content, providing a strong  
 369 negative charge to the polymer chains contributing to the rigidity of their networks [73].  
 370 Mucoadhesion has been described in the case of polymeric excipients as a combination of events  
 371 necessary to explain the adhesion process: hydration of polymer chains, intimate contact with the  
 372 mucus, diffusion and entanglement with mucin fibers, dynamic creation and disruption of labile  
 373 bonds, such as disulfide bridges, electrostatic attractive forces, hydrophobic interactions, hydrogen  
 374 and van der Waals bonds [84]. Several natural (gums, alginates, starch and gelatin), semisynthetic  
 375 (cellulose derivatives, such as methyl-, hydroxypropyl-, hydroxypropylmethyl- and  
 376 carboxymethylcellulose) and fully synthetic polymers (polyacrylates, polymethacrylates,  
 377 crospovidone) have been used to improve nasal delivery of drugs [83]. In the case of N2B transport,  
 378 for example, chitosan and low molecular weight pectins were shown to prolong the residence time  
 379 of nasal formulations in the olfactory region in man [85]. Sodium hyaluronate improved brain  
 380 delivery of a high molecular weight hydrophilic model compound (fluorescein-labeled 4 kDa  
 381 dextran) after nasal administration in rats [86].

382 When these polymers are main constituents or surface-modifiers of nanocarriers, the underlying  
 383 adhesion mechanisms do not change, but the carrier's high surface-area-to-volume ratio translates  
 384 into an extensive interface for more stable and prolonged interactions with the mucus compared to  
 385 larger structures. Besides, size below 500 nm allows nanoparticles to fit in the low viscosity aqueous  
 386 spaces left in-between the mesh of the mucins network, further enhancing the interaction with the  
 387 mucus at molecular level. Finally, positive and hydrophobic surfaces may contribute to maximize  
 388 nanoparticle adhesion towards the mucus, as a consequence of electrostatic attraction and  
 389 hydrophobic interactions with mucins' negatively charged and hydrophobic domains, respectively  
 390 [84]. Some surface modifications, however, reduce mucoadhesion, a characteristic exploited by  
 391 mucus penetrating nanocarriers as discussed in next section of this review (Figure 3).  
 392



393

394 **Figure 3.** Surface chemistry of nanoparticles affecting mucoadhesion (modified with permission from  
 395 [84]).

396 For the above reasons, mucoadhesive nanocarriers have been extensively studied for the N2B  
 397 delivery of drugs.

398 Already in the year 2000, Betbeder and coworkers proposed Biovector™ nanoparticles for the  
 399 nasal delivery of morphine to exploit the direct pathway between the olfactory mucosa and the CNS.  
 400 These maltodextrin-based cationic nanoparticles surrounded by a phospholipid bilayer (average size  
 401  $60 \pm 15$  nm) prolonged morphine antinociceptive activity when co-administered with the opioid drug  
 402 in mice in comparison to morphine solution. Interestingly, the result was not replicated when

403 morphine was administered with a penetration enhancer such as sodium deoxycholate. Despite  
404 morphine was not actually encapsulated in the nanoparticles, it appears that nanoparticles improved  
405 specifically nose-to-brain transport of the opioid, while blood levels were not significantly affected.  
406 This was likely due to the interaction of positive nanoparticle with the nasal mucus layer that may  
407 have increased the formulation residence time and absorption from the olfactory region that is  
408 especially developed in mice [87].

409 In another approach, the group of Silvia Guterres and Adriana Pohlmann developed an  
410 amphiphilic methacrylic copolymer-functionalized poly( $\epsilon$ -caprolactone) nanocapsules as  
411 mucoadhesive system for the N2B delivery of the atypical antipsychotic drug, olanzapine [88].  
412 Nanocapsules showed pH dependent size and surface charge values, ranging from 324.3 to 235.2 nm  
413 and from +55 and +22.7 mV. Nanocapsule/mucin interaction was demonstrated based on increase in  
414 particle size and reduction in nanoparticle concentration using Nanoparticle Tracking Analysis  
415 (NTA). The polymer mucoadhesion was tested both in terms of peak force and work of adhesion and  
416 of prolongation of olanzapine-loaded nanocapsules residence time on porcine nasal mucosa. *In vivo*  
417 studies performed in rats not only confirmed a 1.55 folds higher accumulation of olanzapine in the  
418 brain after nasal administration of mucoadhesive nanoparticles in comparison to a drug solution as  
419 control, but amphiphilic methacrylic copolymer-functionalized poly( $\epsilon$ -caprolactone) nanocapsules  
420 loaded with olanzapine outperformed the controls (drug solution and blank nanocapsules) also in  
421 the pre-pulse inhibition model of cognitive impairment symptoms typical of schizophrenia.  
422 Interestingly, the authors noted that brain accumulation was higher than those reported in literature  
423 for olanzapine-loaded PLGA nanoparticles and attributed the improvement to the cationic  
424 mucoadhesive coating of the nanocapsules [88].

425 Notwithstanding the possibilities provided by new synthetic polymers, polysaccharides have  
426 been amongst the most popular materials used to obtain mucoadhesive nanocarriers. In fact,  
427 polysaccharides appear an ideal choice for the production of nanoparticles to be delivered nasally,  
428 not only because of their mucoadhesive properties, but also for a number of unique characteristics,  
429 such as biomimetic mucosal recognition, well-documented biocompatibility and biodegradability  
430 and ease of chemical modification with targeting moieties. In this regard, polysaccharides can be  
431 incorporated into pharmaceutical nanocarriers in three ways: by absorption to preformed  
432 nanoparticles, by copolymerization or covalent grafting leading to surface modification or by directly  
433 manufacturing polysaccharide-based nanoparticles [89]. For example, albumin nanoparticles  
434 obtained by coacervation and thermal cross-linking, were prepared in presence of  $\beta$ -cyclodextrin  
435 derivatives in order to develop an innovative nasal drug delivery system for the anti-Alzheimer drug  
436 tacrine. The inclusion of  $\beta$ -cyclodextrin derivatives affected drug loading and modulated  
437 nanoparticle mucoadhesiveness. Finally, drug permeation behavior across sheep nasal mucosa from  
438 tacrine-loaded nanoparticles modified with  $\beta$ -cyclodextrin derivatives was increased compared to  
439 nanoparticles based on albumin alone, but it was lower than that obtained with tacrine solution. This  
440 can be explained considering the prolonged release of tacrine observed for nanoparticles [90].

441 Surface-engineered nanostructured lipid carriers coated with *Delonix regia* gum (DRG-NLC) as  
442 a natural mucoadhesive polymer were proposed for the efficient N2B delivery of ondansetron  
443 (OND), a centrally active drug used for the management of chemotherapy induced nausea and  
444 vomiting. The mucoadhesive formulation of OND was produced by high pressure homogenization  
445 using glycerol monostearate and Capryol® 90, as solid and liquid lipids, while soybean lecithin and  
446 poloxamer 188 were used as stabilizers. The nanostructured lipid carriers were subsequently coated  
447 by dispersing OND loaded nanoparticles in a DRG 0.75% w/v aqueous solution. The optimal  
448 nanoparticle formulation showed an average size of 92 nm, a polydispersity index (PDI) of 0.36,  
449 negative surface charge (-11 mV) and acceptable encapsulation efficiency (40% EE, 5.6% drug  
450 loading). Mucoadhesion was assessed *in vitro* by determining a percentage of binding efficiency  
451 between DRG-NLC and mucin (72%). *In vivo* studies carried out in rats showed a brain targeting  
452 efficiency (DTE) of 506% and a direct transport percentage (DTP) of 97% for the intranasal  
453 administration of OND-loaded DRG-NLC using as control the IV injection of a commercial OND IV  
454 formulation (Emeset®). This study, despite the remarkable results, lacked a nasal control (non-

455 mucoadhesive formulation) and did not clarify what was the impact of the presence of free gum, of  
456 non-encapsulated drug, as well as of the processing of nanoparticles (freeze-drying) on the *in vivo*  
457 brain distribution results obtained after DRG-NLC nasal delivery [91].

458 Alginate nanoparticles were produced for the N2B delivery of venlafaxine, a serotonin and  
459 norepinephrine reuptake inhibitor, to treat depression. Alginate nanoparticles were prepared by  
460 ionotropic gelation with calcium ions and subsequent cross-linking with a polycation, such as low  
461 molecular weight chitosan glutamate. Optimized nanoparticles showed an average size slightly  
462 below 175 nm and positive surface charge (+37.4 mV), PDI 0.391, with a high encapsulation efficiency  
463 (81%) and a drug loading of nearly 27%. Mucoadhesion was not studied directly, but *ex vivo*  
464 permeation through porcine nasal mucosa was found to be more than double over 24 hours, when  
465 comparing the venlafaxine-loaded alginate nanoparticles to a drug solution. Forced swimming test  
466 and locomotor activity test were used as behavioral test to assess the efficacy of the nasal  
467 administration of the antidepressant nanoformulation using as controls the drug solution  
468 administered intranasally and a suspension, obtained by crushing commercial tablets, administered  
469 orally. The alginate nanoparticle formulation performed better than the other formulations in the  
470 treatment of depressed animals, even if climbing and immobility parameters were not restored to  
471 levels of naive animals. It has also to be noted that, considering the volume of nanoparticle  
472 suspension administered nasally (100  $\mu$ l), the possible inhalation or swallowing of part of the  
473 nanoformulation could not be excluded. This would eventually provide confounding effects to the  
474 final results. In any case, pharmacokinetics studies conducted using venlafaxine IV administration as  
475 reference and venlafaxine solution administered nasally as control, showed reduced blood levels and  
476 increased brain concentration for the antidepressant drug formulated in alginate nanoparticles. In  
477 particular, DTE and DTP calculated for the venlafaxine-loaded nanocarrier were 426% and 76%,  
478 respectively. An increase in absorption as a consequence of reduced nasal mucociliary clearance,  
479 enhanced mucosal permeation and the modulation of P-gp efflux transporters are some of the factors  
480 explaining the pharmacokinetics data [92]. It is remarkable, however, that the nanoparticle  
481 formulation increased the DTP value only from 63 to 76%, when compared to the nasal solution and  
482 that a significant contribute to the DTE increase came from BBB crossing of the drug after systemic  
483 absorption. This is not unexpected, considering that the antidepressant drug studied is already  
484 marketed as immediate and controlled release tablets and can cross the BBB. As such, the real  
485 improvement of the N2B delivery will consist mainly in the reduction of systemic side effects of the  
486 drug.

487 Among polysaccharides, chitosan, the glucosamine and N-acetyl glucosamine co-polymer  
488 obtained by the deacetylation of chitin, has been demonstrated one of the most promising and  
489 versatile materials for N2B delivery. In fact, chitosan not only is biocompatible, biodegradable,  
490 mucoadhesive and positively charged at nasal slightly acidic pH, but is also an efficient permeation  
491 enhancer able to transiently open the tight junctions of epithelial cells in mucosal tissues [78,93].  
492 Interestingly this feature was demonstrated to be retained when chitosan was used as main  
493 constituent or surface coating for nanocarriers [84,94].

494 Wang and co-workers loaded estradiol in chitosan nanoparticles produced by ionotropic  
495 gelation for nasal administration in view of the treatment of Alzheimer's disease. Chitosan  
496 nanoparticles were obtained using tripolyphosphate anions (TPP) and chitosan with Mw 50,000 Da  
497 in order to obtain nanoparticles with particle size about 270 nm with positive surface charge (+25 mV).  
498 Encapsulation efficiency was around 60% (estradiol concentration 1.9 mg/ml). Smaller (below 100 nm)  
499 or larger (500 nm) nanoparticles could be obtained with Mw 6000 Da and 200,000 Da chitosan,  
500 respectively, but they were not considered suitable for the application. *In vivo* studies in rats showed  
501 a DTE of 320% and DTP of 68% by measuring estradiol concentration in cerebrospinal fluid (CSF)  
502 after IN or IV administration of the estradiol-loaded chitosan nanoparticles. The results were  
503 explained by the ability of chitosan nanoparticle to bind mucins and the improvement of paracellular  
504 transport [95]. However, in these experiments the nasal cavity was isolated from the respiratory and  
505 gastrointestinal tracts, a surgical practice reducing the likelihood of interfering absorption from other  
506 organs but altering retention time and hence absorption from the nasal mucosa. In addition,

507 paracellular transport is not expected to affect significantly the mucosal permeation of highly  
508 lipophilic steroid hormones like estradiol.

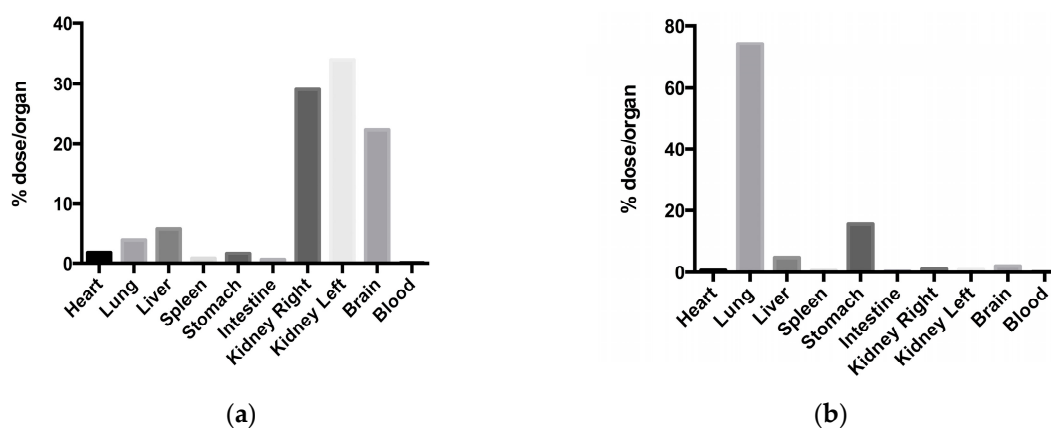
509 Similar chitosan nanoparticles obtained by ionotropic gelation with TPP have been proposed by  
510 several authors for the for the N2B delivery of very different drugs: rivastigmine (size 164 nm, PDI  
511 0.42, EE% 85; DTE 355%, DTP 71%) [96] and thymoquinone (size 103 nm, PDI 0.40, EE%; DTE 3321%  
512 DTP 97%)[97] for Alzheimer's disease, bromocriptine (size 161 nm, PDI 0.44, EE% 84; DTE 630%, DTP  
513 84%) [98], ropinirole (size 171 nm, PDI 0.39, EE% 70; superior brain/blood ratio compared to IN  
514 solution in  $\gamma$ -scintigraphy studies) [99], rasagiline (size 151 nm, PDI 0.38, EE% 96; DTE 325%, DTP  
515 69%) [100] and pramipexole (size 292 nm, PDI 0.29, EE% 93; superior to IN and oral solution in  
516 pharmacodynamics studies) [101] for Parkinson's disease, tapentadol (size 201 nm, PDI 0.20, EE%;  
517 DTE 321%, DTP 69%) for chronic pain management [102]. Despite the different physico-chemical  
518 characteristics of the studied drugs, the results shared striking similarities.

519 Chitosan presents a number of desirable features but also some limitations, for example it is  
520 insoluble at physiologic pH and it is protonated only in acidic conditions, features potentially  
521 interfering with bioadhesion. Hence, several authors adopted nanocarriers based on chitosan  
522 derivatives. Trimethyl chitosan (TMC), for example is a water soluble permanently positively  
523 charged chitosan derivative and was used to encapsulate the analgesic neurotransmitter leucine-  
524 enkefaline (Leu-Enk) by ionotropic gelation. TMC nanoparticles (size 443 nm, PDI 0.32, EE% 78) were  
525 able to increase 35 times the permeability of the peptide across porcine nasal mucosa and produced  
526 a significant increase of the antinociceptive effect in mice after nasal administration during the hot  
527 plate and the acetic acid induced writhing tests [103]. Thiolated chitosan can increase mucoadhesion  
528 via the formation of covalent bonds, such as disulphide bridges, between the thiol groups and mucus  
529 glycoproteins [104]. Cyclobenzaprine (CB) and tizanidine (TZ), two central acting muscle relaxant  
530 used for pain management, were loaded into thiolated chitosan nanoparticles obtained by gelation  
531 with sodium alginate and showed enhanced permeation and reduced toxicity in the RPMI2650 cell  
532 model of human nasal epithelium, increase brain uptake (DTE 2461 and 8523% , DTP 96 and 99% for  
533 CB and TZ, respectively) and significantly enhanced antinociceptive activity for both drugs when  
534 compared to non-thiolated nanoparticles administered nasally [105,106]. In another study, in which  
535 the antidepressant selegiline HCl was encapsulated in thiolated chitosan nanoparticles (215 nm, EE%  
536 70), authors claimed improved anti-inflammatory and neuroprotective effects for the thiolated  
537 polysaccharide itself. In *in vivo* experiments in depression-induced rats, thiolated nanoparticles were  
538 found to be superior to control chitosan nanoparticles when administered at the same dose (10  
539 mg/kg), while providing non-significant differences in the pharmacodynamics effect compared to  
540 controls when the dose administered was halved (5 mg/kg) [107]. In another research, Di Gioia and  
541 co-workers assessed the ability of chitosan derivative nanoparticles to deliver dopamine to the  
542 striatum. Glycol chitosan, a water-soluble derivative of chitosan, was used to manufacture  
543 nanoparticles by ionotropic gelation with TPP along with sulfobutylether- $\beta$ -cyclodextrin to improve  
544 dopamine loading. When administered nasally as a single dose nanoparticles did not modify brain  
545 levels of the neurotransmitter, but repeated intranasal administration significantly increased  
546 dopamine levels in the ipsilateral striatum [108].

547 It is worth mentioning that in almost all these promising studies, the nanocarriers improved the  
548 performance of drugs that already showed N2B transport when administered nasally with traditional  
549 liquid formulations such solutions.

550 In alternative formulation approaches chitosan is used as a surface modifier of carriers made of  
551 other materials. The water soluble antipsychotic chlorpromazine HCl was loaded into chitosan  
552 grafted PLGA nanoparticles in view of nasal treatment of schizophrenia to provide brain targeting  
553 and sustained release of drug, decrease the dose and administration frequency and reduce side effects.  
554 PLGA nanoparticles were prepared with a combined self-assembly/nanoprecipitation method in  
555 presence of dextran sulphate, followed by the grafting of the chitosan on PLGA nanoparticles surface.  
556 The selected formulation, characterized by an average size 464 nm (PDI 0.19) and 37% encapsulation  
557 efficiency, showed good mucoadhesion on sheep nasal mucosa and provided a permeation of  
558 chlorpromazine of 9% over 4 hours, controlled by the release kinetics of the PLGA nanoparticles (40%

559 release over 48 hours) [109]. Liposomes coated with a chitosan derivative were proposed for the nasal  
 560 administration of ghrelin. Ghrelin is a centrally acting peptide hormone able to stimulate food intake  
 561 and for this reason a potential drug for the treatment of cachexia the wasting pathologic syndrome  
 562 associated to some chronic diseases, such as cancers, hearth or kidneys failure. Ghrelin loaded  
 563 liposomes were prepared by the lipid film re-hydration/extrusion technique followed by coating with  
 564 N-([2-hydroxy-3-trimethylammonium]propyl) chitosan chloride (size 194 nm, PDI 0.19, EE% 56). The  
 565 chitosan coated liposomes bound mucin more efficiently than uncoated anionic liposomes (63% *vs.*  
 566 40%) and improved permeation through a Calu-3 cell monolayer used as model of the upper airways  
 567 epithelial barrier (10.8% *vs.* 3.6% anionic liposome *vs.* 0% free peptide) [110]. Finally, Clementino and  
 568 co-workers developed hybrid chitosan/lipid nanocapsules for the N2B delivery of simvastatin.  
 569 Statins have been suggested as potential neuroprotective drugs, in reason of their pleiotropic effects,  
 570 *i.e.* anti-inflammatory, antioxidant and immunomodulatory actions [111,112]. The particles obtained  
 571 by the self-assembly of a mixture of phospholipids and liquid lipids in presence of chitosan aqueous  
 572 solution. The nanocapsules obtained not only showed small particle size (200 nm), positive surface  
 573 charge and high encapsulation efficiency, but were shown to be efficiently biodegraded by enzymes  
 574 present in nasal secretions such as lysozyme to provide a more efficient release of the drug at the  
 575 deposition site on nasal mucosa. Gamma scintigraphy studies evidenced a significantly higher brain  
 576 accumulation of the isotope (above 20% of the administered radioactivity) after IN administration of  
 577 simvastatin loaded nanocapsules in rats in comparison to the IN administration of a <sup>99m</sup>Tc-labelled  
 578 suspension of the statin (Figure 4) [113].  
 579



580 **Figure 4.** Fraction of total radioactivity recovered per organ 90 minutes after the nasal administration  
 581 in rats of (a) <sup>99m</sup>Tc-labelled simvastatin-loaded nanoparticles; (b) <sup>99m</sup>Tc-labelled simvastatin  
 582 suspension [113].

583 In recent years, several studies have proposed the inclusion of nanoformulations, often  
 584 micro/nanoemulsions, lipid or polymer nanoparticles, within mucoadhesive gels (xantan gum,  
 585 chitosan) [114,115] or *in situ* gelling preparations obtained with thermosensitive (poloxamers 407)  
 586 [116], pH sensitive (Carbopol 934) [117] and ion sensitive (gellan gum) [118,119] polymers. Even if  
 587 the approach is seemingly appealing (combination of nanoparticle encapsulation/protection within  
 588 viscous medium able to prolong residence time), the gel matrix viscosity might result in hindered  
 589 nanoparticles migration, poor interaction with the nasal mucosa as well as low drug release. In  
 590 addition, the superiority over more traditional formulation solutions is open to question.

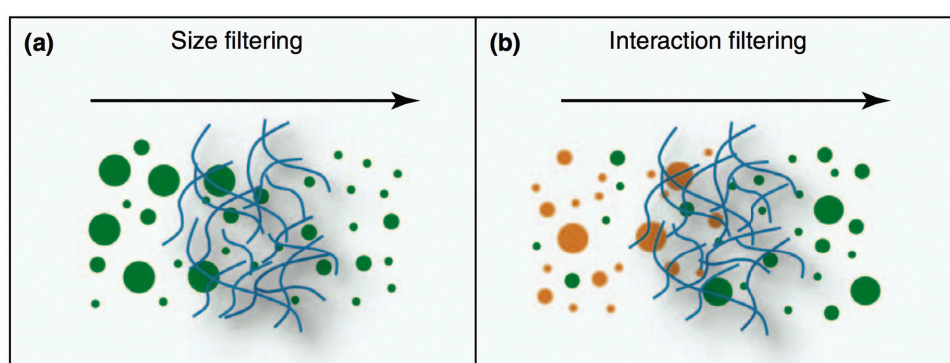
591 In summary, mucoadhesive nanoparticles have been one of the most explored platforms for the  
 592 N2B delivery of drugs. Results are supporting in all cases a superiority of the mucoadhesive  
 593 nanoformulation over drug solutions administered nasally and/or intravenously, although a limited  
 594 number of studies focus on direct comparison with potential competing formulation approaches such  
 595 as liquid or even solid formulations containing mucoadhesive or permeation enhancing excipients.  
 596  
 597

## 598 4. Beyond bioadhesion: mucus penetrating and penetration enhancing nanocarriers

### 599 4.1. Mucus penetrating nanocarriers

600 The popular mucoadhesive approach has been in recent years challenged by the evidence of the  
601 multiple barrier properties provided by the presence of the mucus layer. The mucus physiologic  
602 function relies on it acting as a dynamic semipermeable barrier via two major mechanisms working  
603 together: interaction filtering and size filtering (Figure 5) [120].

604 Interaction filtering occurs for molecules, supramolecular structures and particles,  
605 independently of their size. This phenomenon limits diffusion through the mucus via direct non-  
606 specific interactions, such as electrostatic, hydrogen and hydrophobic binding, with glycosylated,  
607 non-glycosylated regions of mucins as well as with lipid components of mucus. These interactions  
608 have been evidenced for charged and/or hydrophilic molecules, lipophilic drugs, peptides and  
609 proteins [121].  
610



611  
612 **Figure 5.** Major mechanisms hindering particles from diffusing through mucus: (a) Size filtering, only  
613 particles smaller than the mesh openings of the mucin fibers network are allowed to cross, whereas  
614 larger objects are blocked; (b) Interaction filtering, particles behavior is different according to surface  
615 properties: particles (orange) interacting strongly with the components of the mucus gel are trapped,  
616 whereas particles (green) showing weak interactions are allowed to cross (reproduced with  
617 permission from [121]).

618 Mucus is a dense molecular network with a characteristic mesh spacing that prevents larger  
619 particles diffusion through it. This mesh spacing has been reported to vary from 20 up to 200-500 nm  
620 from various authors [120,122].

621 Hence, it has been hypothesized that the use of nanocarriers with a sufficiently small size and  
622 coated with polymers that minimize interactions with mucins such as poly(ethylene) glycol (PEG)  
623 may increase mucus diffusivity and favor the close contact with the underlying epithelium.  
624 Interestingly, already in 2004 the group of Maria José Alonso observed that when fluorescent labelled  
625 PEG-PLA nanoparticles were administered intranasally in rats, the presence of PEG, smaller size (175  
626 nm) and higher PEG coating density were the properties favoring the accumulation of particles  
627 within rat nasal mucosa [123]. Later, a group at John Hopkins University demonstrated using  
628 multiple particle tracking that 100 and 200 nm particles coated with high density of low MW PEG (2  
629 or 5 kDa) were able to rapidly penetrate human respiratory [124] and chronic rhinosinusitis mucus  
630 [125] and designed mucus penetrating PEG-PLGA nanoparticles [126,127]. However, those results  
631 were not replicated in experiments in which PEG-coated magnetic nanoparticles despite showing  
632 decreased adhesion to mucus components failed to penetrate through native respiratory mucus even  
633 in presence of a magnetic field [128].

634 Diazepam and midazolam, two benzodiazepines in use for the treatment of *status epilepticus*,  
635 were encapsulated in PLGA nanoparticles coated with poloxamers 407 (Pluronic® F127), a block co-  
636 polymer surfactant previously reported to enhance mucus penetration of nanoparticles [125]. In both  
637 research works optimal particles showed size below 200 nm, moderately negative surface potential  
638 ( $\zeta$  potential between -15 and -30 mV), controlled drug permeation kinetics across sheep nasal mucosa,

639 direct brain transport (DTP around 60%) and superior brain targeting efficiency compared to drug  
640 solution after nasal administration in rats (235-260 % *vs.* 125-160% DTE) [51,129]. In these papers,  
641 however, the authors did not claim or study the mucus penetration of the produced particles, but the  
642 nanocarrier characteristics match those of mucus penetrating carriers.

643 Recently, Sekerdag and collaborators proposed lipid/PEG-PLGA nanoparticles as mucus  
644 penetrating carriers of farnesylthiosalicylic acid (FTA) for a non-invasive nose-to-brain treatment of  
645 glioblastoma. The nanoparticles produced (size 163 nm, PDI 0.19, surface charge -12 mV, EE% >95%)  
646 were demonstrated after nasal administration to significantly reduce tumor volume (55% reduction  
647 as evidenced by MRI analysis) induced by implanting RG2 cells in the rat brain. The antitumor effect  
648 obtained was comparable to that obtained by nanoparticles administered intravenously. The  
649 biodistribution studies evidenced that the percentage of the dose attaining the brain was 0.04% ID/g  
650 for both formulations, but in the case of the nasal administration the amount of the dose accumulating  
651 in liver and spleen was significantly reduced, suggesting a superior safety profile for the nasal  
652 administration of the nanocarrier [130].

653 It is interesting to note that in some cases PEG-coated nanoparticles have been used as  
654 mucoadhesive carriers [131], but this is due to the fine tuning of the particle size and coating  
655 characteristic necessary to obtain particles able to slip through the mucus layer [132]. Furthermore,  
656 PEG coating has been associated with reduced interactions with epithelial cells and as a consequence  
657 reduced uptake, for the same exact reasons related to mucus penetration, *i.e.* reduced interactions  
658 with proteins and biomolecules [133,134]. It appears clear that mucus penetrating particles have not  
659 been yet sufficiently studied in nose-to-brain delivery and that more robust studies have to  
660 demonstrate the validity of the concept in terms of improved targeting of the CNS compared to other  
661 surface modification approaches.  
662

#### 663 4.2. Penetration enhancing nanocarriers

664 In alternative to mucus penetrating “stealth” particles, some authors have developed particles  
665 in which components can act as penetration enhancers. In reality, this classification is often  
666 superimposed to others (chitosan for example acts both as mucoadhesive agent and as penetration  
667 enhancer), but for the purpose of this review penetration enhancing particles will be considered those  
668 made of components, often surfactants, claimed to have the power to alter the barrier properties of  
669 the nasal mucosa.

670 For example, zolmitriptan and sumatriptan, two selective serotonin agonists in use for the  
671 treatment of acute migraine, were encapsulated into micelles composed of PEG 400, benzyl alcohol,  
672 Vitamin E TPGS, Pluronic® F127 and Trascutol P®. In particular, Trascutol P®, *i.e.* diethylene glycol  
673 monoethyl ether, and Vitamin E TPGS were used to solubilize and enhance the absorption of drugs  
674 through the nasal mucosa [135]. The micelles exhibited size below 25 nm, significantly increased  
675 triptan delivery to the brain (up to 3-7% of the administered dose) compared to IN or IV drug solution  
676 and did not show signs of local toxicity also after prolonged nasal administration in comparison to  
677 controls (28 days) [136,137].

678 Olanzapine-loaded nanocubic vesicles, obtained by incorporating the surface-active triblock  
679 copolymer poloxamer 188 (consisting of a hydrophobic polypropylene oxide block capped with  
680 hydrophilic polyethylene oxide moieties) in phosphatidylcholine bilayers, were compared to the  
681 corresponding liposomes in biodistribution studies in rats after nasal delivery. The nanocubic  
682 vesicles (size 363 nm, PDI 0.088, EE% 67) improved absolute bioavailability (37.9 *vs.* 14.9%) and DTE  
683 (100 *vs.* 80%) compared to the control liposomal formulation. The improvement was attributed to the  
684 presence of poloxamers in the formulation imparting both higher elasticity and penetration  
685 enhancing properties to vesicles [138]. In this study, one of the few using LC-MS/MS to quantify the  
686 drug in the biodistribution studies, the nanocarrier nasal delivery was not superior to the IV control  
687 in delivering the drug to the brain, as evidenced by the value of DTE. Also in the work of  
688 Albdelrahman and co-workers elasticity of spanlastics nanovesicles was claimed to be the mechanism  
689 improving the N2B delivery of the antipsychotic drug risperidone. Spanlastics vesicles, produced by

690 injecting a Span 60 and risperidone ethanol solution in a PVA aqueous solution (size 103 nm, PDI  
691 0.34, EE% 64), exhibited relatively high Newtonian viscosity, improved permeation through *ex vivo*  
692 nasal sheep mucosa and improved brain accumulation of the drug in comparison to drug solution  
693 (DTE 469% *vs.* 217 %). However, DTP was superior for the nasal solution (55 % *vs.* 79 %) as spanlastics  
694 significantly improved systemic absorption of the drug [139].

695 Gelatin nanostructured lipid carriers were used to deliver to the brain the neurotrophic factor,  
696 basic fibroblast growth factor (bFGF), suggested protecting dopaminergic neurons in Parkinson's  
697 disease, via the non-invasive nasal route. The gelatin nanoparticles were prepared by a water-in-  
698 water emulsion in presence of poloxamer 188 and phospholipids, crosslinking with glyceraldehyde  
699 following by freeze-drying (size 172 nm, PDI 0.210,  $\zeta$ -potential -38 mV, EE% 87). The nasal  
700 administration of the gelatin NLC significantly increased exogenous bFGF in olfactory bulb and  
701 striatum without influencing the integrity to nasal mucosa. The surface modified nanocarriers  
702 outperformed control gelatin nanoparticles also in studies with hemiparkinsonian rats inducing  
703 functional recovery after IN but not after IV administration. This was attributed to the presence of  
704 poloxamers 188 and its ability to reduce the barrier of mucus layer altering its viscosity and to  
705 enhance permeation by interacting and perturbing lipid membranes and/or modulating tight  
706 junctions [140]. Polysorbate 80 (Tween 80) was claimed to have similar effects in SLN loaded with  
707 rosmarinic acid obtained using glyceryl monostearate (GMS) and hydrogenated soy  
708 phosphatidylcholine. These particles were designed to manage the symptoms of Huntington's  
709 disease. Polysorbate 80 coated SLN improved behavioral abnormalities and attenuated the oxidative  
710 stress in 3-nitropropionic acid treated rats to greater extent than rosmarinic acid administered  
711 intranasally or the same nanoparticles injected intravenously [141].

712 Fatty acids have been traditionally indicated as absorption promoting agents in nasal delivery  
713 [142]. Recently, zolmitriptan has been formulated in novasomes, *i.e.* nanovesicular fatty acid enriched  
714 structures. The optimized novasomes formulated with a combination of Span® 80, cholesterol and  
715 stearic acid (size 150 nm, PDI 0.48,  $\zeta$ -potential -38 mV, EE% 93), showed an enhanced brain  
716 accumulation ( $C_{\max}$  1.27 % ID/g) with a direct transport percentage of 99.2% when compared with the  
717 intravenous drug solution. The effects were attributed to the potential disruption of the nasal  
718 membrane and to the ability of these vesicles to "squeeze" themselves through the olfactory  
719 epithelium opening [143]. The actual contribution of this last mechanism to the nose-to-brain delivery  
720 is far from being supported by actual data demonstrating such ability to transfer across the nasal  
721 mucosa of elastic vesicles. Similarly, the occlusive effect claimed by other authors for nasally  
722 delivered alprazolam SLN appears highly unlikely [144].

723 In general, penetration enhancing nanocarriers studies lack of a fundamental control that is  
724 administration of a conventional formulation of the same drug containing the penetration enhancer  
725 alone. Only demonstrating a superior nose-to-brain delivery over this formulation of the use of  
726 nanocarriers would be fully warranted.

727

## 728 5. Targeting the Nasal Epithelium for Optimizing the Nose to Brain Delivery

729 Undoubtedly, one of the most fascinating aspects of the pharmaceutical nanotechnology is the  
730 so called "active" targeting of nanoparticles, *i.e.* the recognition of cells or tissues affected by the  
731 disease by means of surface ligands able to interact specifically with receptors and/or other  
732 biomolecules present on the biologic target. To deliver specifically the therapeutic dose of the drug  
733 where it has to act, avoiding side effects and with optimal therapeutic efficacy, has been the Grail  
734 Quest of pharmacotherapy since the dawn of modern pharmaceutical sciences [145].

735 As pointed out by an excellent paper by Alexander Florence, several obstacles (often  
736 underestimated or disregarded by scientist) are present *in vivo* for targeted nanocarriers (nanocarrier  
737 aggregation, premature drug release from the carrier, uptake by reticuloendothelial system, delivery  
738 off-target, degradation) and those have actually hindered the successful translation of targeted  
739 approach of drug delivery systems to clinical settings [146].

740 In the case of nose-to-brain delivery the approach is interestingly not directed to the delivery of  
741 the particles themselves to a specific cell or receptor within the CNS, but to the interaction with cells  
742 of the nasal region more likely to favor the translocation to the brain, *i.e.* the olfactory epithelium.  
743 Several surface ligands have been proposed, but two strategies emerge as the most studied in recent  
744 years: lectins and cell penetrating peptides targeted nanocarriers.

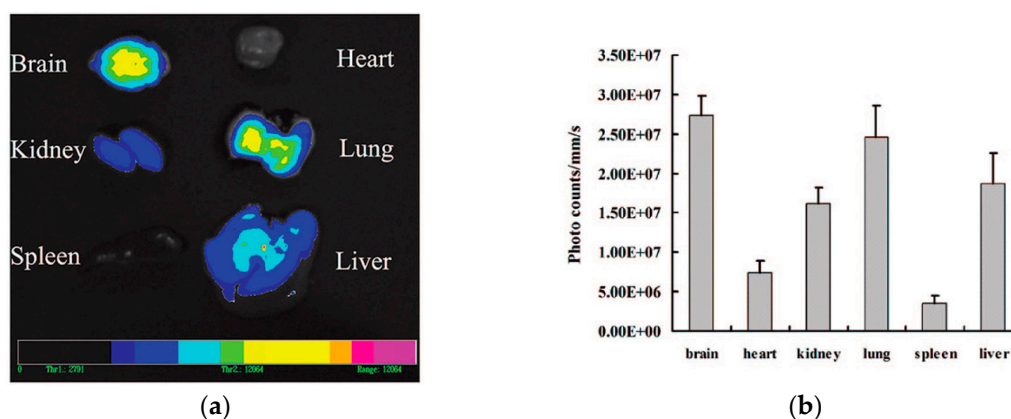
#### 745 5.1. Lectin-modified nanocarriers

746 Lectins are proteins or glycoproteins extracted from plants able to recognize and bind with high  
747 level of specificity glycan arrays of glycosylated lipids and proteins present on the surface of different  
748 cell types. For this reason, since 1988 they have been proposed as targeting ligands for drug delivery  
749 systems, initially in order to obtain absorption enhancement in the gastrointestinal tract [147].  
750 However, the potential of lectins for nose-to-brain delivery has been demonstrated qualitatively and  
751 quantitatively in two seminal works by Broadwell and Balin [148] and Thorne *et al.* [149]. In those  
752 works, it has been demonstrated that wheat germ agglutinin (WGA)/horseradish peroxidase  
753 conjugate (62 kDa) can bind the cell surface of olfactory sensory cells, undergo adsorptive endocytosis  
754 and anterograde axonal transport and eventually accumulate in the olfactory bulb at concentrations  
755 (140 nM) more than 100 folds that those obtained by IV administration of the same conjugate and 700  
756 folds those attained by the enzyme not conjugated to WGA. In fact, WGA obtained from *Triticum*  
757 *vulgare* specifically bind to N-acetyl-D-glucosamine and sialic acid residues abundantly present in  
758 nasal structures. As a consequence, WGA has been the most explored targeting ligand for  
759 nanocarriers for nose-to-brain delivery.

760 WGA was conjugated to PEG-PLA nanoparticles to obtain 85-90 nm targeted nanoparticles  
761 loaded with the fluorescent dye 6-coumarin. WGA targeted nanoparticles administered intranasally  
762 improved both blood (1.4 folds) and brain (2 folds) concentrations of the fluorescent dye when  
763 compared to plain PEG-PLA nanoparticles, without appreciable nasal ciliotoxicity [150]. Other  
764 studies in which WGA-conjugated PEG-PLA were radiolabelled with <sup>125</sup>I revealed that that  
765 nanoparticles after nasal administration in rats were rapidly (5-30 min) transported to the CNS via  
766 the extracellular pathway along olfactory and especially trigeminal nerves, while cerebrospinal fluid  
767 appeared to contribute to a small extent to the process [151].

768 The same group from the Fudan University of Shanghai (PR China) incorporate vasoactive intestinal  
769 peptide (VIP), a neuroprotective peptide potentially useful in a number of neurodegenerative  
770 disorders including AD in WGA conjugated PEG-PLA nanoparticles (size 100-120 nm, EE% 70, drug  
771 loading% 1.4). In biodistribution studies, 30-50% of radioactively labelled VIP was found in the CNS  
772 and WGA-conjugated targeted improved brain targeting (5.66-7.71 folds increase) compared to non-  
773 targeted PLA nanoparticles (3.57-4.74 folds increase) and control VIP solution administered nasally  
774 in mice. Furthermore, in an *in vivo* model of cholinergic impairment, VIP loaded WGA-NP induced  
775 improvement in spatial memory of rats at lower doses compared to non-targeted nanoparticles (12.5  
776 *vs.* 25 µg/kg) [152]. In a subsequent work, WGA-targeted PEG-PLA nanoparticles were loaded with  
777 quantum dots in order to develop specific brain imaging agents for CNS diseases. Once again, the  
778 brain targeting capacity of the WGA was demonstrated with a relative fluorescence intensity detected  
779 three hours after nasal administration in mice (40 mg/kg, 5 µl each nostril) ranked as follows: brain  
780 ≥ lung > liver > kidney > heart > spleen (Figure 6) [153].

781



782 **Figure 6.** Distribution of WGA-conjugated quantum dots-loaded nanoparticles in various organs  
 783 following intranasal administration 3 h after dosing: (a) optical image (b) quantification of  
 784 luminescence signals (adapted with permission from [153]. Copyright 2008 American Chemical  
 785 Society).

786 PEG-PLA or PEG-PLGA nanoparticles were conjugated to other lectins, such as *Solanum tuberosum*  
 787 lectin (STL), binding to N-acetylglucosamine [154], Ulex europeus agglutinin I (UEA I) and  
 788 odorranalectin (OL), both binding to L-fucose largely present on the olfactory epithelium [155,156].  
 789 STL-functionalized PEG-PLGA nanoparticles loaded with haloperidol (size 132 nm, PDI 0.174,  $\zeta$ -  
 790 potential -14 mV, EE% 73, DL% 0.85) increased the brain tissue haloperidol concentrations after nasal  
 791 administration by 1.5–3-fold compared to non-STL-functionalized particles and other routes of  
 792 administration [157].

793 Since one of the major problems of lectins is their immunogenicity, being odorranalectin the smallest  
 794 peptide with lectin-like activity, it was identified as a potential targeting ligand with reduced  
 795 immunogenicity. OL-conjugated PEG-PLG nanoparticles were loaded with peptide urocortin  
 796 reported to be able to restore nigrostriatal function in PD (size 115 nm, PDI 0.193, EE% 75, DL% 0.14).  
 797 The *in vivo* studies in hemiparkinsonian rats evidenced a better improvement of the symptoms  
 798 related to the dopaminergic lesion for OL-conjugated nanoparticles compared to control treatments  
 799 and this was shown to be related to a partial but not complete recovery of monoamine  
 800 neurotransmitters levels [158].

801 Despite this recent advancement, the use of lectins still faces criticism related to the potential toxicity  
 802 and immunogenicity, making mandatory a toxicological assessment of the targeted carrier both  
 803 systemically and locally towards the nasal epithelial surface and the CNS [159].  
 804

## 805 5.2. Cell penetrating peptides as surface ligands for targeted nanocarriers

806 Cell penetrating peptides (CPPs) are short cationic sequences of amino acids able to cross cell  
 807 membranes and translocate to intracellular space similarly to their model, *i.e.* the HIV transactivator  
 808 of transcription (Tat) protein [160]. CPPs have been shown to be unspecific to cell-type and able to  
 809 translocate various cargos (small molecules, proteins, nucleic acids, nanocarriers) across different  
 810 biological barriers such as intestinal wall, BBB, skin [161].

811 These characteristics make CPPs attractive as ligands for nose-to-brain delivery of nanocarriers.  
 812 In the already cited study by Gartzandia, the conjugation of CPPs (Tat or Penetratin) to the surface  
 813 of polymer and especially of lipid-based nanoparticles improved their ability to cross an *in vitro*  
 814 primary rat olfactory cell monolayer model [67]. In another study, PEG-PLA nanoparticles  
 815 functionalized with low molecular weight protamine were found to accumulate in 16HBE14o- human  
 816 bronchial epithelial cells at a greater extent than unmodified particles and after loading with the  
 817 fluorescence dye coumarin-6 and nasal administration to rats increased fluorescence signal in various  
 818 brain structures more than two folds compared to unmodified particles [162]. In a similar set of  
 819 experiments, micelles obtained using Tat conjugated to methoxy poly(ethylene glycol)-poly( $\epsilon$ -

820 caprolactone) (mPEG-PCL) amphiphilic block copolymers and loaded with coumarin accumulated  
821 more than original micelles in C6 rat glioma cells and in rats bearing C6 tumors intracranially. In the  
822 latter *in vivo* experiment, no difference was found in fluorescence brain distribution 1h after nasal  
823 administration between micelles. However, after 4 hours, while fluorescence signal decreased for  
824 unmodified micelles, it increased in animals treated with Tat conjugated mPEG-PCL micelles,  
825 probably due to their greater ability to penetrate intracellularly [163]. In subsequent works, the same  
826 group from Tokyo University of Pharmacy and Life Sciences loaded the above-mentioned micelles  
827 with camptothecin in view of treating brain tumors and with small-interferin RNA (siRNA) for the  
828 suppression of genes involved in CNS disorders. Camptothecin-loaded Tat-mPEG-PCL micelles (size  
829 88.5 nm,  $\zeta$ -potential +10 mV, EE% 62) showed C6 higher cytotoxic effect on rat glioma cells *in vitro*  
830 compared to micelles not modified with the CPP and, more interestingly, after nasal administration  
831 prolonged survival of rats bearing intracranial C6 glioma (including 1 long term survivor) compared  
832 to the control micelles and drug solution (1.2 mg/kg, once-a-day for one week) [164]. In the case of  
833 siRNA, the nucleic acid was condensed with Tat-mPEG-PCL to obtain polyplexes of 50-100 nm. Brain  
834 distribution studies after nasal administration, carried out loading Alexa-dextran 10 kDa as model of  
835 siRNA in micelles, evidenced an increase in brain accumulation in comparison to controls (IV Tat-  
836 mPEG-PCL micelles or IN mPEG-PCL micelles) due to Tat-promoted permeation of the nasal mucosa  
837 and increased uptake within olfactory and trigeminal nerves [165].  
838 Despite the impressive translocation abilities, CPPs have some drawbacks such as sequestration in  
839 endosomes, limited intracellular localization profiles and lack efficient transport to the cytoplasm  
840 [160]. These drawbacks have prompted the development of different delivery approaches.  
841 For example, the group of Paolo Giunchedi from University of Sassari designed a drug delivery  
842 system for N2B delivery of the complex of the 29-amino-acid peptide derived from the rabiesvirus  
843 glycoprotein (RVG) with siRNA interfering with the expression of BACE1, the  $\beta$  secretase responsible  
844 for the processing of amyloid precursor protein in  $\beta$  amyloid peptide, the main constituent of  
845 extracellular plaques hallmark of AD. The RVG-siRNA complex was loaded in SLN coated with  
846 chitosan and preliminary experiments showed an improved crossing of CaCo-2 cells monolayer by  
847 RVG-siRNA formulated in SLN and especially in chitosan-coated SLN, compared to the naked  
848 complex. In this approach, the mucoadhesive nanocarrier has to protect the complex and help it cross  
849 the nasal mucosal barrier to allow interaction of RVG cell penetrating peptide with acetylcholine  
850 receptors located at the trigeminal nerve ending and olfactory bulb. This approach has to still be  
851 validated with *in vivo* experiments [166].  
852

### 853 5.3. Other targeting approaches

854 Several other ligands have been indicated to be potentially useful to enhance nose-to-brain  
855 delivery and in this section some examples are provided of the most interesting approaches  
856 alternative to lectins and cell penetrating peptides.

857 One of the early approaches for targeted drug delivery, suggested also for other administration  
858 routes, has been the use of viral vectors. Frenken and Solomon adopted filamentous bacteriophages  
859 as vector for the nasal administration of anti- $\beta$  amyloid (A $\beta$ ) antibodies designed for the monitoring  
860 of amyloid plaques of living AD patients. The bacteriophage f88 was genetically engineered to encode  
861 on its surface protein III, a single-chain antibody constructed from variable sections of light and heavy  
862 chains of anti- A $\beta$  IgM 508 antibody. After three daily nasal administrations of the filamentous  
863 bacteriophage vector, amyloid plaques were successfully targeted and visualized fluorescent-labeled  
864 antiphage antibodies in the olfactory bulb and the hippocampus region of transgenic mice carrying  
865 a double mutation in the amyloid precursor protein (APP). The crossing of the nasal barrier was  
866 attributed to the linear structure of the phage, previously demonstrated to provide penetration  
867 properties in various membranes. The lack of spreading to other brain sections suggested a transport  
868 via the olfactory neurons. The vector was proven inert and non-toxic, despite one of the possible  
869 drawbacks of viral vectors could be the trigger of immune defense mechanisms such as the activation

870 of microglia scavenger cells [167]. Interestingly, the approach is the object of a filed patent application  
871 [168].

872 Lactoferrin (Lf), a natural iron-binding cationic glycoprotein of the transferrin family, has been  
873 used as targeting ligand on the surface of nanocarriers as Lf receptor has been demonstrated to be  
874 highly expressed on the surface of respiratory epithelial cells as well as on neurons and brain  
875 endothelial cells [168]. For this reason, lactoferrin modified PEG-PCL nanoparticles were developed  
876 to enable brain delivery following intranasal administration of the neuroprotective NAP peptide, a  
877 fragment of the activity-dependent neuroprotective protein. Nanoparticles were prepared using  
878 emulsion/solvent evaporation technique followed by conjugation with thiolated Lf (size 88 nm, PDI  
879 0.22,  $\zeta$ -potential -24 mV, EE% 48, DL% 0.62). The Lf targeted nanoparticles not only increased brain  
880 accumulation more than two folds compared to unmodified nanoparticles, but showed improved  
881 neuroprotective effects in an AD model, *i.e.* mice intracerebroventricularly co-injected with ibotenic  
882 acid and  $\beta$ -amyloid<sub>1-40</sub>, as shown by behavioral experiments such as the Morris water maze task. This  
883 was found to be related to an amelioration of the impaired cholinergic neurotransmission via a  
884 reduction in acetylcholinesterase activity and reduced depletion of choline acetyltransferase  
885 [169,170]. The same targeting strategy was successfully adopted for rotigotine-loaded PEG-PLGA  
886 nanoparticles for PD treatment [171] and for mPEG-PLA nanoparticles encapsulating  $\alpha$ -asarone, a  
887 drug extracted from the traditional Chinese medicine herb *Acorus tatarinowii* Schott and recently  
888 proposed for the treatment of epilepsy [172].

889 PEG-PLA nanoparticles loaded with the analgesic peptide  $\alpha$ -cobrotoxin were modified with  
890 OX26 antibodies to target transferrin receptors present in the BBB after nasal administration (size 96  
891 nm, PDI 0.11,  $\zeta$ -potential -33 mV, EE% 82). Results showed that brain delivery of the peptide labelled  
892 with fluorescein isothiocyanate was enhanced by the intranasal delivery of nanoparticles in  
893 comparison with intramuscular administration and that the enhancement was more pronounced in  
894 the case of antibody targeted nanoparticles. The peptide solution could barely penetrate the brain.  
895 Despite the authors attributed this to an appreciable capacity of the nanoparticles to cross the BBB,  
896 the actual mechanism of transport hypothesized, *i.e.* intact nanoparticles crossing the nasal mucosa,  
897 entering capillaries and finally crossing untouched the BBB, was not supported by clear experimental  
898 evidence [173].

899 Finally, in an interesting approach from the group of Rodney Ho of the University of  
900 Washington (USA) liposomes targeted with the integrin-targeting ligand Arg-Gly-Asp (RGD) were  
901 coupled with a pressurized olfactory drug (POD) delivery device to improve nose-to-brain  
902 administration of the analgesic opioid fentanyl. RGD can increase binding and enhance permeability  
903 across epithelial cells expressing  $\alpha_v\beta_3$  integrins, thus fentanyl-loaded liposomes integrating the  
904 palmitoylated peptide (size 96 nm, PDI 0.11, EE% 80) were used to enhance residence time and  
905 absorption of the nasally administered opioid. The POD intranasal delivery device is a new device  
906 enabling preferential deposition of the aerosolized formulation on the olfactory region. Experiments  
907 demonstrated that RGD-conjugated liposomes could withstand the aerosolization with POD device  
908 without size change, phospholipid bilayer disruption or impairment of the targeting. Interestingly,  
909 when liposomes were administered to rats using POD device, fentanyl plasma concentrations as well  
910 as those measured in the brain 5 minutes post-administration were inferior (although not  
911 significantly different) to those obtained using free fentanyl. However, when the analgesic effect was  
912 measured, the fentanyl-loaded RGD liposomes provided a slightly slower onset of action and lower  
913 but more prolonged analgesic effect [174]. The decisions to combine the use of a device that is  
914 designed for an optimal deposition in human nasal cavity and the adoption of small animals for *in*  
915 *vivo* studies appear questionable. A larger animal model such as sheep would suit more the testing  
916 of nasal devices.

917

## 918 6. Future perspectives of nose-to-brain delivery with nanocarriers

919 Nose-to-brain delivery is a fascinating scientific topic. In the quest to achieve a non-invasive,  
920 efficient, safe and potentially disruptive innovation in the field of treatment of CNS disorders and

921 brain diseases, the application of nanocarriers appears an asset, with several advantages but also few  
922 risks to be addressed early-on in the medicinal product development. Despite the promising results  
923 with several drugs, different materials and targeting approaches, to the best of our knowledge not a  
924 single one is actively developed by a pharmaceutical company to transfer the technology from the  
925 laboratory to the clinical stage. Several reasons are behind the lack of translational research successes  
926 for nanomedicines, some of which are related to the manufacturing scale-up, safety and quality  
927 challenges related to these non-biological complex medicinal products in general. Some reasons are  
928 however to be pinpointed in some shortcomings of the scientific works that in several cases  
929 highlighted the potential overlooking the weak points of the approach or the more pertinent controls  
930 necessary to demonstrate superiority over “traditional” formulation approaches. Furthermore, too  
931 often the drugs selected are already able to cross the BBB at some extent and/or produce CNS  
932 pharmacological effects, thus for these nanoencapsulation improve the only performance.  
933 Nanomedicines, especially in the case of a sensitive application such as the therapy of CNS  
934 conditions, are not required to *improve*, but to *enable* therapies that would not be possible without the  
935 application of nanoencapsulation [175].

936 For these reasons, in the planning of future nose-to-brain research protocols applying  
937 nanocarriers for the formulation of the drug, the rigorous and methodical pharmaceutical scientist  
938 should take in to account the following points in order to demonstrate the superiority of the designed  
939 nanomedicines and provide the data necessary for further development of a medicinal product:

- 940 • Select a potent drug with unfavorable physico-chemical characteristics for N2B;
- 941 • Design particles with biocompatible, biodegradable, GRAS materials;
- 942 • Adopt a robust, validated and up scalable fabrication method;
- 943 • Determine drug release from nanocarrier in biorelevant conditions;
- 944 • Establish early-on the safety and biodegradability pattern of the nanocarrier;
- 945 • If possible/advisable, adopt particles with size 100-400 nm, as smaller particles are more  
946 likely to enter the CNS with consequent concerns related to the nanotoxicology of those  
947 materials;
- 948 • Develop bioanalytical methods able to detect the drug instead of fluorescent or  
949 radioactive labels in biodistribution studies, if possible;
- 950 • Develop methods allowing to track the particles in the tissues in order to differentiate  
951 free drug and nanomaterial biodistribution;
- 952 • Carry out the *in vivo* experiments perfusing the organs before dissection, in order to  
953 eliminate blood contamination from the analytical quantitation;
- 954 • Establish the pharmacokinetics of free and nanoencapsulated drug, applying multiple  
955 and relevant controls (IV and IN administered solutions or formulations including  
956 absorption promoting excipients);
- 957 • Determine relevant parameters such as drug targeting efficiency (DTE) and direct  
958 transport percentage (DTP);
- 959 • Establish the therapeutic proof of concept through pharmacodynamics studies in a  
960 disease model as close as possible to the human condition;
- 961 • Combine PK and PD data to critically predict the feasibility of the treatment in terms of  
962 drug dose, amount of formulation to be administered, posology etc.;
- 963 • Select the candidate formulation for pre-clinical/clinical development.

964  
965 In conclusion, nose-to-brain delivery evolved from a series of interesting observations looked upon  
966 with skepticism to a promising, although challenging, field of research. Nanomedicines appears to  
967 be a pivotal tool to enable the brain delivery of potent drug unable to cross the BBB and when used  
968 as such they will fulfill the potential demonstrated in the many scientific studies conducted so far.  
969

970 **Acknowledgments:** F Sonvico, AR Pohlmann and SS Guterres would like to acknowledge the Brazilian  
971 government as recipients of CNPq grants in the programs “Ciências sem Fronteiras” (BOLSA PESQUISADOR  
972 VISITANTE ESPECIAL – PVE 401196/2014–3) and “Produtividade em Pesquisa”.

973 **Conflicts of Interest:** The authors declare no conflict of interest.

974

975 **References**

- 976 1. Pozzoli, M.; Rogueda, P.; Zhu, B.; Smith, T.; Young, P. M.; Traini, D.; Sonvico, F. Dry powder nasal drug  
977 delivery: challenges, opportunities and a study of the commercial Teijin Puvlizer Rhinocort device and  
978 formulation. *Drug Dev Ind Pharm* **2016**, *42*, 1660–1668.
- 979 2. Pires, A.; Fortuna, A.; Alves, G.; Falcão, A. Intranasal drug delivery: how, why and what for? *J Pharm Pharm*  
980 *Sci* **2009**, *12*, 288–311.
- 981 3. Chen, Y.; Liu, L. Modern methods for delivery of drugs across the blood-brain barrier. *Adv Drug Deliv Rev*  
982 **2012**, *64*, 640–665.
- 983 4. Gabathuler, R. Approaches to transport therapeutic drugs across the blood-brain barrier to treat brain  
984 diseases. *Neurobiol Dis* **2010**, *37*, 48–57.
- 985 5. Garcia-Garcia, E.; Gil, S.; Andrieux, K.; Desmaële, D.; Nicolas, V.; Taran, F.; Georgin, D.; Andreux, J. P.;  
986 Roux, F.; Couvreur, P. A relevant in vitro rat model for the evaluation of blood-brain barrier translocation  
987 of nanoparticles. *Cell Mol Life Sci* **2005**, *62*, 1400–1408.
- 988 6. Alam, M. I.; Beg, S.; Samad, A.; Baboota, S.; Kohli, K.; Ali, J.; Ahuja, A.; Akbar, M. Strategy for effective brain  
989 drug delivery. *Eur J Pharm Sci* **2010**, *40*, 385–403.
- 990 7. Wong, H. L.; Wu, X. Y.; Bendayan, R. Nanotechnological advances for the delivery of CNS therapeutics. *Adv*  
991 *Drug Deliv Rev* **2012**, *64*, 686–700.
- 992 8. Costantino, L.; Boraschi, D. Is there a clinical future for polymeric nanoparticles as brain-targeting drug  
993 delivery agents? *Drug Discov Today* **2012**, *17*, 367–378.
- 994 9. Pardeshi, C. V.; Belgamwar, V. S. Direct nose to brain drug delivery via integrated nerve pathways  
995 bypassing the blood-brain barrier: an excellent platform for brain targeting. *Expert Opin Drug Deliv* **2013**,  
996 *10*, 957–972.
- 997 10. Thorne, R. G.; Pronk, G. J.; Padmanabhan, V.; Frey, W. H. Delivery of insulin-like growth factor-I to the rat  
998 brain and spinal cord along olfactory and trigeminal pathways following intranasal administration.  
999 *Neuroscience* **2004**, *127*, 481–496.
- 1000 11. Chapman, C. D.; Frey, W. H.; Craft, S.; Danielyan, L.; Hallschmid, M.; Benedict, C. Intranasal treatment of  
1001 central nervous system dysfunction in humans. *Pharm Res* **2013**, *30*, 2475–2484.
- 1002 12. Illum, L. Transport of drugs from the nasal cavity to the central nervous system. *Eur J Pharm Sci* **2000**, *11*, 1–  
1003 18.
- 1004 13. Ying, W. The nose may help the brain: intranasal drug delivery for treating neurological diseases. *Future*  
1005 *Neurology* **2008**, *3*, 1–4.
- 1006 14. Dhuria, S. V. Intranasal delivery to the central nervous system: mechanisms and experimental  
1007 considerations. *J Pharm Sci* **2010**, *99*, 1654–1673.
- 1008 15. Samaridou, E.; Alonso, M. J. Nose-to-brain peptide delivery - The potential of nanotechnology. *Bioorg Med*  
1009 *Chem* **2018** (in press).
- 1010 16. Comfort, C.; Garrastazu, G.; Pozzoli, M.; Sonvico, F. Opportunities and Challenges for the Nasal  
1011 Administration of Nanoemulsions. *Curr Top Med Chem* **2015**, *15*, 356–368.
- 1012 17. Cady, R. A novel intranasal breath-powered delivery system for sumatriptan: a review of technology and  
1013 clinical application of the investigational product AVP-825 in the treatment of migraine. *Expert Opin Drug*  
1014 *Deliv* **2015**, *12*, 1565–1577.
- 1015 18. Yamada, K.; Hasegawa, M.; Kametani, S.; Ito, S. Nose-to-brain delivery of TS-002, prostaglandin D2  
1016 analogue. *J Drug Target* **2007**, *15*, 59–66.

- 1017 19. Colombo, G.; Lorenzini, L.; Zironi, E.; Galligioni, V.; Sonvico, F.; Sonvico, F.; Balducci, A. G.; Balducci, A.  
1018 G.; Pagliuca, G.; Giuliani, A.; Calzà, L.; Scagliarini, A. Brain distribution of ribavirin after intranasal  
1019 administration. *Antiviral Res* **2011**, *92*, 408–414.
- 1020 20. Van Woensel, M.; Wauthoz, N.; Rosière, R.; Amighi, K.; Mathieu, V.; Lefranc, F.; Van Gool, S. W.; De  
1021 Vleeschouwer, S. Formulations for intranasal delivery of pharmacological agents to combat brain disease:  
1022 A new opportunity to tackle GBM? *Cancers (Basel)* **2013**, *5*, 1020–1048.
- 1023 21. Peterson, A.; Bansal, A.; Hofman, F.; Chen, T. C.; Zada, G. A systematic review of inhaled intranasal  
1024 therapy for central nervous system neoplasms: An emerging therapeutic option. *J Neurooncol* **2014**, *116*,  
1025 437–446.
- 1026 22. Duchi, S.; Ovadia, H.; Touitou, E. Nasal administration of drugs as a new non-invasive strategy for efficient  
1027 treatment of multiple sclerosis. *J Neuroimmunol.* **2013**, *258*, 32–40.
- 1028 23. Kulkarni, J. A.; Avachat, A. M. Pharmacodynamic and pharmacokinetic investigation of cyclodextrin-  
1029 mediated asenapine maleate in situ nasal gel for improved bioavailability. *Drug Dev Ind Pharm* **2017**, *43*,  
1030 234–245.
- 1031 24. Aly, A. E.-E.; Waszczak, B. L. Intranasal gene delivery for treating Parkinsons disease: Overcoming the  
1032 blood-brain barrier. *Expert Opin Drug Deliv* **2015**, *12*, 1923–1941.
- 1033 25. Sood, S.; Jain, K.; Gowthamarajan, K. Intranasal therapeutic strategies for management of Alzheimer's  
1034 disease. *J Drug Target* **2014**, *22*, 279–294.
- 1035 26. Yuan, D.; Yi, X.; Zhao, Y.; Poon, C.-D.; Bullock, K. M.; Hansen, K. M.; Salameh, T. S.; Farr, S. A.; Banks, W.  
1036 A.; Kabanov, A. V. Intranasal delivery of N-terminal modified leptin-pluronic conjugate for treatment of  
1037 obesity. *J Control Release* **2017**, *263*, 172–184.
- 1038 27. Arora, P.; Sharma, S.; Garg, S. Permeability issues in nasal drug delivery. *Drug Discov Today* **2002**, *7*, 967–  
1039 975.
- 1040 28. Merkus, F. W. H. M.; van den Berg, M. P. Can Nasal Drug Delivery Bypass the??Blood-Brain Barrier? *Drugs*  
1041 *in R & D* **2007**, *8*, 133–144.
- 1042 29. Illum, L. Is nose-to-brain transport of drugs in man a reality? *J Pharm Pharmacol* **2004**, *56*, 3–17.
- 1043 30. Djupesland, P. G. Nasal drug delivery devices: characteristics and performance in a clinical perspective-a  
1044 review. *Drug Deliv Transl Res* **2012**, *3*, 42–62.
- 1045 31. Kozlovskaya, L.; Stepensky, D. Quantitative analysis of drug delivery to the brain via nasal route. *J Control*  
1046 *Release* **2014**, *189*, 133–140.
- 1047 32. Ruigrok, M. J. R.; de Lange, E. C. M. Emerging Insights for Translational Pharmacokinetic and  
1048 Pharmacokinetic-Pharmacodynamic Studies: Towards Prediction of Nose-to-Brain Transport in Humans.  
1049 *AAPS J* **2015**, *17*, 493–505.
- 1050 33. Reger, M. A.; Watson, G. S.; Green, P. S.; Wilkinson, C. W.; Baker, L. D.; Cholerton, B.; Fishel, M. A.;  
1051 Plymate, S. R.; Breitner, J. C. S.; DeGroodt, W.; Mehta, P.; Craft, S. Intranasal insulin improves cognition  
1052 and modulates beta-amyloid in early AD. *Neurology* **2008**, *70*, 440–448.
- 1053 34. Craft, S.; Claxton, A.; Baker, L. D.; Hanson, A. J.; Cholerton, B.; Trittschuh, E. H.; Dahl, D.; Caulder, E.;  
1054 Neth, B.; Montine, T. J.; Jung, Y.; Maldjian, J.; Whitlow, C.; Friedman, S. Effects of Regular and Long-Acting  
1055 Insulin on Cognition and Alzheimer's Disease Biomarkers: A Pilot Clinical Trial. *J Alzheimers Dis* **2017**, *57*,  
1056 1325–1334.
- 1057 35. Quintana, D. S.; Westlye, L. T.; Hope, S.; Nærland, T.; Elvsåshagen, T.; Dørum, E.; Rustan, Ø.; Valstad, M.;  
1058 Rezvaya, L.; Lishaugen, H.; Stensønes, E.; Yaqub, S.; Smerud, K. T.; Mahmoud, R. A.; Djupesland, P. G.;  
1059 Andreassen, O. A. Dose-dependent social-cognitive effects of intranasal oxytocin delivered with novel

- 1060 Breath Powered device in adults with autism spectrum disorder: a randomized placebo-controlled double-  
1061 blind crossover trial. *Transl Psychiatry* **2017**, *7*, e1136.
- 1062 36. Macdonald, K.; Feifel, D. Helping oxytocin deliver: considerations in the development of oxytocin-based  
1063 therapeutics for brain disorders. *Front Neurosci* **2013**, *7*, 35.
- 1064 37. Gozes, I.; Morimoto, B. H.; Tiong, J.; Fox, A.; Sutherland, K.; Dangoor, D.; Holser-Cochav, M.; Vered, K.;  
1065 Newton, P.; Aisen, P. S.; Matsuoka, Y.; Van Dyck, C. H.; Thal, L. NAP: Research and development of a  
1066 peptide derived from activity-dependent neuroprotective protein (ADNP). *CNS Drug Rev* **2005**, *11*, 353–  
1067 368.
- 1068 38. Morimoto, B. H.; Schmechel, D.; Hirman, J.; Blackwell, A.; Keith, J.; Gold, M.; AL-108-211 Study A double-  
1069 blind, placebo-controlled, ascending-dose, randomized study to evaluate the safety, tolerability and effects  
1070 on cognition of AL-108 after 12 weeks of intranasal administration in subjects with mild cognitive  
1071 impairment. *Dement Geriatr Cogn Disord* **2013**, *35*, 325–336.
- 1072 39. Boxer, A. L.; Lang, A. E.; Grossman, M.; Knopman, D. S.; Miller, B. L.; Schneider, L. S.; Doody, R. S.; Lees,  
1073 A.; Golbe, L. I.; Williams, D. R.; Corvol, J.-C.; Ludolph, A.; Burn, D.; Lorenzl, S.; Litvan, I.; Roberson, E. D.;  
1074 Höglinger, G. U.; Koestler, M.; Jack, C. R.; Van Deerlin, V.; Randolph, C.; Lobach, I. V.; Heuer, H. W.;  
1075 Gozes, I.; Parker, L.; Whitaker, S.; Hirman, J.; Stewart, A. J.; Gold, M.; Morimoto, B. H.; AL-108-231  
1076 Investigators Davunetide in patients with progressive supranuclear palsy: a randomised, double-blind,  
1077 placebo-controlled phase 2/3 trial. *Lancet Neurol* **2014**, *13*, 676–685.
- 1078 40. Landis, M. S.; Boyden, T.; Pegg, S. Nasal-to-CNS drug delivery: where are we now and where are we  
1079 heading? An industrial perspective. *Ther Deliv* **2012**, *3*, 195–208.
- 1080 41. Kürti, L.; Gáspár, R.; Márki, Á.; Kápolna, E.; Bocsik, A.; Veszeka, S.; Bartos, C.; Ambrus, R.; Vastag, M.;  
1081 Deli, M. A.; Szabó-Révész, P. In vitro and in vivo characterization of meloxicam nanoparticles designed for  
1082 nasal administration. *Eur J Pharm Sci* **2013**, *50*, 86–92.
- 1083 42. Bartos, C.; Ambrus, R.; Sipos, P.; Budai-Szűcs, M.; Csányi, E.; Gáspár, R.; Márki, Á.; Seres, A. B.; Sztojkov-  
1084 Ivanov, A.; Horváth, T.; Szabó-Révész, P. Study of sodium hyaluronate-based intranasal formulations  
1085 containing micro- or nanosized meloxicam particles. *Int J Pharm* **2015**, *491*, 198–207.
- 1086 43. Abdelbary, G. A.; Tadros, M. I. Brain targeting of olanzapine via intranasal delivery of core-shell  
1087 difunctional block copolymer mixed nanomicellar carriers: In vitro characterization, ex vivo estimation of  
1088 nasal toxicity and in vivo biodistribution studies. *Int J Pharm* **2013**, *452*, 300–310.
- 1089 44. Nour, S. A.; Abdelmalak, N. S.; Naguib, M. J.; Rashed, H. M.; Ibrahim, A. B. Intranasal brain-targeted  
1090 clonazepam polymeric micelles for immediate control of status epilepticus: in vitro optimization, ex vivo  
1091 determination of cytotoxicity, in vivo biodistribution and pharmacodynamics studies. *Drug Deliv* **2016**, *23*,  
1092 3681–3695.
- 1093 45. Arumugam, K.; Subramanian, G. S.; Mallayasamy, S. R.; Averineni, R. K.; Reddy, M. S.; Udupa, N. A study  
1094 of rivastigmine liposomes for delivery into the brain through intranasal route. *Acta Pharm* **2008**, *58*, 287–297.
- 1095 46. Gupta, S.; Kesarla, R.; Chotai, N.; Misra, A.; Omri, A. Systematic Approach for the Formulation and  
1096 Optimization of Solid Lipid Nanoparticles of Efavirenz by High Pressure Homogenization Using Design of  
1097 Experiments for Brain Targeting and Enhanced Bioavailability. *Biomed Res Int* **2017**, *2017*, 5984014–18.
- 1098 47. Fatouh, A. M.; Elshafeey, A. H.; Abdelbary, A. Intranasal agomelatine solid lipid nanoparticles to enhance  
1099 brain delivery: Formulation, optimization and in vivo pharmacokinetics. *Drug Des Devel Ther* **2017**, *11*,  
1100 1815–1825.

- 1101 48. Alam, T.; Pandit, J.; Vohora, D.; Aqil, M.; Ali, A.; Sultana, Y. Optimization of nanostructured lipid carriers  
1102 of lamotrigine for brain delivery: in vitro characterization and in vivo efficacy in epilepsy. *Expert Opin Drug*  
1103 *Deliv* **2014**, *12*, 181–194.
- 1104 49. Khan, A.; Imam, S. S.; Aqil, M.; Ahad, A.; Sultana, Y.; Ali, A.; Khan, K. Brain Targeting of Temozolomide  
1105 via the Intranasal Route Using Lipid-Based Nanoparticles: Brain Pharmacokinetic and Scintigraphic  
1106 Analyses. *Mol Pharm* **2016**, *13*, 3773–3782.
- 1107 50. Kubek, M. J.; Domb, A. J.; Veronesi, M. C. Attenuation of Kindled Seizures by Intranasal Delivery of  
1108 Neuropeptide-Loaded Nanoparticles. *Neurotherapeutics* **2009**, *6*, 359–371.
- 1109 51. Sharma, D.; Sharma, R. K.; Sharma, N.; Gabrani, R.; Sharma, S. K.; Ali, J.; Dang, S. Nose-To-Brain Delivery  
1110 of PLGA-Diazepam Nanoparticles. *AAPS PharmSciTech* **2015**, *16*, 1108–1121.
- 1111 52. Ahmad, N.; Ahmad, I.; Umar, S.; Iqbal, Z.; Samim, M.; Ahmad, F. J. PNIPAM nanoparticles for targeted and  
1112 enhanced nose-to-brain delivery of curcuminoids: UPLC/ESI-Q-ToF-MS/MS-based pharmacokinetics and  
1113 pharmacodynamic evaluation in cerebral ischemia model. *Drug Deliv* **2016**, *23*, 2095–2114.
- 1114 53. Wong, L. R.; Ho, P. C. Role of serum albumin as a nanoparticulate carrier for nose-to-brain delivery of R-  
1115 flurbiprofen: implications for the treatment of Alzheimer's disease. *J Pharm Pharmacol* **2018**, *70*, 59–69.
- 1116 54. Win-Shwe, T.-T.; Sone, H.; Kurokawa, Y.; Zeng, Y.; Zeng, Q.; Nitta, H.; Hirano, S. Effects of PAMAM  
1117 dendrimers in the mouse brain after a single intranasal instillation. *Toxicol Lett* **2014**, *228*, 207–215.
- 1118 55. Lungare, S.; Hallam, K.; Badhan, R. K. S. Phytochemical-loaded mesoporous silica nanoparticles for nose-  
1119 to-brain olfactory drug delivery. *Int J Pharm* **2016**, *513*, 280–293.
- 1120 56. Mahajan, H. S.; Mahajan, M. S.; Nerkar, P. P.; Agrawal, A. Nanoemulsion-based intranasal drug delivery  
1121 system of saquinavir mesylate for brain targeting. *Drug Deliv* **2014**, *21*, 148–154.
- 1122 57. Mistry, A.; Stolnik, S.; Illum, L. Nanoparticles for direct nose-to-brain delivery of drugs. *Int J Pharm* **2009**,  
1123 *379*, 146–157.
- 1124 58. Kozlovskaya, L.; Stepensky, D. Quantitative analysis of the brain-targeted delivery of drugs and model  
1125 compounds using nano-delivery systems. *J Control Release* **2013**, *171*, 17–23.
- 1126 59. Md, S.; Mustafa, G.; Baboota, S.; Ali, J. Nanoneurotherapeutics approach intended for direct nose to brain  
1127 delivery. *Drug Dev Ind Pharm* **2015**, *41*, 1922–1934.
- 1128 60. Pires, P. C.; Santos, A. O. Nanosystems in nose-to-brain drug delivery\_ A review of non-clinical brain  
1129 targeting studies. **2018**, *270*, 89–100.
- 1130 61. Feng, Y.; He, H.; Li, F.; Lu, Y.; Qi, J.; Wu, W. An update on the role of nanovehicles in nose-to-brain drug  
1131 delivery. *Drug Discov Today* **2018**.
- 1132 62. Kulkarni, A. D.; Vanjari, Y. H.; Sancheti, K. H.; Belgamwar, V. S.; Surana, S. J.; Pardeshi, C. V.  
1133 Nanotechnology-mediated nose to brain drug delivery for Parkinson's disease: a mini review. *J Drug Target*  
1134 **2015**, *23*, 775–788.
- 1135 63. Fonseca-Santos, B.; Gremião, M. P. D.; Chorilli, M. Nanotechnology-based drug delivery systems for the  
1136 treatment of Alzheimer's disease. *Int J Nanomedicine* **2015**, *10*, 4981–5003.
- 1137 64. Marianecchi, C.; Rinaldi, F.; Hanieh, P. N.; Paolino, D.; Marzio, L. D.; Carafa, M. Nose to Brain Delivery:  
1138 New Trends in Amphiphile-Based "Soft" Nanocarriers. *Curr Pharm Des* **2015**, *21*, 5225–5232.
- 1139 65. Kanazawa, T. Brain delivery of small interfering ribonucleic acid and drugs through intranasal  
1140 administration with nano-sized polymer micelles. *Med Devices (Auckl)* **2015**, *8*, 57–64.
- 1141 66. Selvaraj, K.; Gowthamarajan, K.; Karri, V. V. S. R. Nose to brain transport pathways an overview: potential  
1142 of nanostructured lipid carriers in nose to brain targeting. *Artif Cells Nanomed Biotechnol* **2017**, *7*, 1–8.

- 1143 67. Gartzandia, O.; Egusquiaguirre, S. P.; Bianco, J.; Pedraz, J. L.; Igartua, M.; Hernandez, R. M.; Pr at, V.;  
1144 Beloqui, A. Nanoparticle transport across in vitro olfactory cell monolayers. *Int J Pharm* **2016**, *499*, 81–89.
- 1145 68. Yang, M.; Lai, S. K.; Yu, T.; Wang, Y.-Y.; Happe, C.; Zhong, W.; Zhang, M.; Anonuevo, A.; Fridley, C.;  
1146 Hung, A.; Fu, J.; Hanes, J. Nanoparticle penetration of human cervicovaginal mucus: the effect of polyvinyl  
1147 alcohol. *J Control Release* **2014**, *192*, 202–208.
- 1148 69. Musumeci, T.; Pellitteri, R.; Spatuzza, M.; Puglisi, G. Nose-to-brain delivery: Evaluation of polymeric  
1149 nanoparticles on olfactory ensheathing cells uptake. *J Pharm Sci* **2014**, *103*, 628–635.
- 1150 70. Murali, K.; Kenesei, K.; Li, Y.; Demeter, K.; K ornyei, Z.; Madar asz, E. Uptake and bio-reactivity of  
1151 polystyrene nanoparticles is affected by surface modifications, ageing and LPS adsorption: In vitro studies  
1152 on neural tissue cells. *Nanoscale* **2015**, *7*, 4199–4210.
- 1153 71. Mistry, A.; Stolnik, S.; Illum, L. Nose-to-Brain Delivery: Investigation of the Transport of Nanoparticles  
1154 with Different Surface Characteristics and Sizes in Excised Porcine Olfactory Epithelium. *Mol Pharm* **2015**,  
1155 *12*, 2755–2766.
- 1156 72. Mistry, A.; Glud, S. Z.; Kjems, J.; Randel, J.; Howard, K. A.; Stolnik, S.; Illum, L. Effect of physicochemical  
1157 properties on intranasal nanoparticle transit into murine olfactory epithelium. *J Drug Target* **2009**, *17*, 543–  
1158 552.
- 1159 73. Lai, S. K.; Wang, Y.-Y.; Hanes, J. Mucus-penetrating nanoparticles for drug and gene delivery to mucosal  
1160 tissues. *Adv Drug Deliv Rev* **2009**, *61*, 158–171.
- 1161 74. Xu, Q.; Ensign, L. M.; Boylan, N. J.; Sch on, A.; Gong, X.; Yang, J.-C.; Lamb, N. W.; Cai, S.; Yu, T.; Freire, E.;  
1162 Hanes, J. Impact of Surface Polyethylene Glycol (PEG) Density on Biodegradable Nanoparticle Transport in  
1163 Mucus ex Vivo and Distribution in Vivo. *ACS Nano* **2015**, *9*, 9217–9227.
- 1164 75. Ahmad, E.; Feng, Y.; Qi, J.; Fan, W.; Ma, Y.; He, H.; Xia, F.; Dong, X.; Zhao, W.; Lu, Y.; Wu, W. Evidence of  
1165 nose-to-brain delivery of nanoemulsions: Cargoes but not vehicles. *Nanoscale* **2017**, *9*, 1174–1183.
- 1166 76. Kanazawa, T.; Kaneko, M.; Niide, T.; Akiyama, F.; Kakizaki, S.; Ibaraki, H.; Shiraiishi, S.; Takashima, Y.;  
1167 Suzuki, T.; Seta, Y. Enhancement of nose-to-brain delivery of hydrophilic macromolecules with stearate- or  
1168 polyethylene glycol-modified arginine-rich peptide. *Int J Pharm* **2017**, *530*, 195–200.
- 1169 77. Gabal, Y. M.; Kamel, A. O.; Sasmour, O. A.; Elshafeey, A. H. Effect of surface charge on the brain delivery  
1170 of nanostructured lipid carriers in situ gels via the nasal route. *Int J Pharm* **2014**, *473*, 442–457.
- 1171 78. Casettari, L.; Illum, L. Chitosan in nasal delivery systems for therapeutic drugs. *J Control Release* **2014**, *190C*,  
1172 189–200.
- 1173 79. Lucchini, R. G.; Dorman, D. C.; Elder, A.; Veronesi, B. Neurological impacts from inhalation of pollutants  
1174 and the nose-brain connection. *NeuroToxicology* **2012**, *33*, 838–841.
- 1175 80. Karmakar, A.; Zhang, Q.; Zhang, Y. Neurotoxicity of nanoscale materials. *J Food Drug Anal* **2014**, *22*, 147–  
1176 160.
- 1177 81. Simk o, M.; Mattsson, M. O. Risks from accidental exposures to engineered nanoparticles and neurological  
1178 health effects: A critical review. *Part Fibre Toxicol* **2010**, *7*, 42.
- 1179 82. Marttin, E.; Schipper, N. G. M.; Coos Verhoef, J.; Merkus, F. W. H. M. Nasal mucociliary clearance as a  
1180 factor in nasal drug delivery. *Adv Drug Deliv Rev* **1998**, *29*, 13–38.
- 1181 83. Ugwoke, M. I.; Agu, R. U.; Verbeke, N.; Kinget, R. Nasal mucoadhesive drug delivery: background,  
1182 applications, trends and future perspectives. *Adv Drug Deliv Rev* **2005**, *57*, 1640–1665.
- 1183 84. Sosnik, A.; Neves, das, J.; Sarmiento, B. Mucoadhesive polymers in the design of nano-drug delivery  
1184 systems for administration by non-parenteral routes: A review. *Prog Polym Sci* **2014**, *39*, 2030–2075.

- 1185 85. Charlton, S.; Jones, N. S.; Davis, S. S.; Illum, L. Distribution and clearance of bioadhesive formulations from  
1186 the olfactory region in man: effect of polymer type and nasal delivery device. *Eur J Pharm Sci* **2007**, *30*, 295–  
1187 302.
- 1188 86. Horvát, S.; Fehér, A.; Wolburg, H.; Sipos, P.; Veszelka, S.; Tóth, A.; Kis, L.; Kurunczi, A.; Balogh, G.; Kürti,  
1189 L.; Eros, I.; Szabó-Révész, P.; Deli, M. A. Sodium hyaluronate as a mucoadhesive component in nasal  
1190 formulation enhances delivery of molecules to brain tissue. *Eur J Pharm Biopharm* **2009**, *72*, 252–259.
- 1191 87. Betbeder, D.; Spérandio, S.; Latapie, J. P.; de Nadai, J.; Etienne, A.; Zajac, J. M.; Francés, B. Biovector  
1192 nanoparticles improve antinociceptive efficacy of nasal morphine. *Pharm Res* **2000**, *17*, 743–748.
- 1193 88. Fonseca, F. N.; Betti, A. H.; Carvalho, F. C.; Gremião, M. P. D.; Dimer, F. A.; Guterres, S. S.; Tebaldi, M. L.;  
1194 Rates, S. M. K.; Pohlmann, A. R. Mucoadhesive amphiphilic methacrylic copolymer-functionalized poly( $\epsilon$ -  
1195 caprolactone) nanocapsules for nose-to-brain delivery of olanzapine. *J Biomed Nanotechnol* **2014**, *11*, 1472–  
1196 1481.
- 1197 89. Lemarchand, C.; Gref, R.; Couvreur, P. Polysaccharide-decorated nanoparticles. *Eur J Pharm Biopharm* **2004**,  
1198 *58*, 327–341.
- 1199 90. Luppi, B.; Bigucci, F.; Corace, G.; Delucca, A.; Cerchiara, T.; Sorrenti, M.; Catenacci, L.; Di Pietra, A. M.;  
1200 Zecchi, V. Albumin nanoparticles carrying cyclodextrins for nasal delivery of the anti-Alzheimer drug  
1201 tacrine. *Eur J Pharm Sci* **2011**, *44*, 559–565.
- 1202 91. Devkar, T. B.; Tekade, A. R.; Khandelwal, K. R. Surface engineered nanostructured lipid carriers for  
1203 efficient nose to brain delivery of ondansetron HCl using Delonix regia gum as a natural mucoadhesive  
1204 polymer. *Colloids Surf B Biointerfaces* **2014**, *122*, 143–150.
- 1205 92. Haque, S.; Md, S.; Fazil, M.; Kumar, M.; Sahni, J. K.; Ali, J.; Baboota, S. Venlafaxine loaded chitosan NPs for  
1206 brain targeting: pharmacokinetic and pharmacodynamic evaluation. *Carbohydr Polym* **2012**, *89*, 72–79.
- 1207 93. Deli, M. A. Potential use of tight junction modulators to reversibly open membranous barriers and improve  
1208 drug delivery. *Biochim Biophys Acta* **2009**, *1788*, 892–910.
- 1209 94. Vllasaliu, D.; Exposito-Harris, R.; Heras, A.; Casettari, L.; Garnett, M.; Illum, L.; Stolnik, S. Tight junction  
1210 modulation by chitosan nanoparticles: comparison with chitosan solution. *Int J Pharm* **2010**, *400*, 183–193.
- 1211 95. Wang, X.; He, H.; Leng, W.; Tang, X. Evaluation of brain-targeting for the nasal delivery of estradiol by the  
1212 microdialysis method. *Int J Pharm* **2006**, *317*, 40–46.
- 1213 96. Fazil, M.; Md, S.; Haque, S.; Kumar, M.; Baboota, S.; Sahni, J. K.; Ali, J. Development and evaluation of  
1214 rivastigmine loaded chitosan nanoparticles for brain targeting. *Eur J Pharm Sci* **2012**, *47*, 6–15.
- 1215 97. Alam, S.; Khan, Z. I.; Mustafa, G.; Kumar, M.; Islam, F.; Bhatnagar, A.; Ahmad, F. J. Development and  
1216 evaluation of thymoquinone-encapsulated chitosan nanoparticles for nose-to-brain targeting: a  
1217 pharmacoscintigraphic study. *Int J Nanomedicine* **2012**, *7*, 5705–5718.
- 1218 98. Md, S.; Khan, R. A.; Mustafa, G.; Chuttani, K.; Baboota, S.; Sahni, J. K.; Ali, J. Bromocriptine loaded chitosan  
1219 nanoparticles intended for direct nose to brain delivery: Pharmacodynamic, Pharmacokinetic and  
1220 Scintigraphy study in mice model. *Eur J Pharm Sci* **2013**, *48*, 393–405.
- 1221 99. Jafarieh, O.; Md, S.; Ali, M.; Baboota, S.; Sahni, J. K.; Kumari, B.; Bhatnagar, A.; Ali, J. Design,  
1222 characterization, and evaluation of intranasal delivery of ropinirole-loaded mucoadhesive nanoparticles for  
1223 brain targeting. *Drug Dev Ind Pharm* **2015**, *41*, 1674–1681.
- 1224 100. Mittal, D.; Md, S.; Hasan, Q.; Fazil, M.; Ali, A.; Baboota, S.; Ali, J. Brain targeted nanoparticulate drug  
1225 delivery system of rasagiline via intranasal route. *Drug Deliv* **2014**, *23*, 130–139.

- 1226 101. Raj, R.; Wairkar, S.; Sridhar, V.; Gaud, R. Pramipexole dihydrochloride loaded chitosan nanoparticles for  
1227 nose to brain delivery: Development, characterization and in vivo anti-Parkinson activity. *Int J Biol*  
1228 *Macromol* **2017**, *109*, 27–35.
- 1229 102. Javia, A.; Thakkar, H. Intranasal delivery of tapentadol hydrochloride-loaded chitosan nanoparticles:  
1230 formulation, characterisation and its in vivo evaluation. *J Microencapsul* **2017**, *34*, 644–658.
- 1231 103. Kumar, M.; Pandey, R. S.; Patra, K. C.; Jain, S. K.; Soni, M. L.; Dangi, J. S.; Madan, J. Evaluation of  
1232 neuropeptide loaded trimethyl chitosan nanoparticles for nose to brain delivery. *Int J Biol Macromol* **2013**,  
1233 *61*, 189–195.
- 1234 104. Shahnaz, G.; Vetter, A.; Barthelmes, J.; Rahmat, D.; Laffleur, F.; Iqbal, J.; Perera, G.; Schlocker, W.;  
1235 Dünnhaupt, S.; Augustijns, P.; Bernkop-Schnürch, A. Thiolated chitosan nanoparticles for the nasal  
1236 administration of leuprolide: bioavailability and pharmacokinetic characterization. *Int J Pharm* **2012**, *428*,  
1237 164–170.
- 1238 105. Patel, D.; Naik, S.; Misra, A. Improved transnasal transport and brain uptake of tizanidine HCl-loaded  
1239 thiolated chitosan nanoparticles for alleviation of pain. *J Pharm Sci* **2012**, *101*, 690–706.
- 1240 106. Patel, D.; Naik, S.; Chuttani, K.; Mathur, R.; Mishra, A. K.; Misra, A. Intranasal delivery of cyclobenzaprine  
1241 hydrochloride-loaded thiolated chitosan nanoparticles for pain relief. *J Drug Target* **2013**, *21*, 759–769.
- 1242 107. Singh, D.; Rashid, M.; Hallan, S. S.; Mehra, N. K.; Prakash, A.; Mishra, N. Pharmacological evaluation of  
1243 nasal delivery of selegiline hydrochloride-loaded thiolated chitosan nanoparticles for the treatment of  
1244 depression. *Artif Cells Nanomed Biotechnol* **2016**, *44*, 865–877.
- 1245 108. Di Gioia, S.; Trapani, A.; Mandracchia, D.; De Giglio, E.; Cometa, S.; Mangini, V.; Arnesano, F.; Belgiovine,  
1246 G.; Castellani, S.; Pace, L.; Lavecchia, M. A.; Trapani, G.; Conese, M.; Puglisi, G.; Cassano, T. Intranasal  
1247 delivery of dopamine to the striatum using glycol chitosan/sulfobutylether- $\beta$ -cyclodextrin based  
1248 nanoparticles. *Eur J Pharm Biopharm* **2015**, *94*, 180–193.
- 1249 109. Chalikwar, S. S.; Mene, B. S.; Pardeshi, C. V.; Belgamwar, V. S.; Surana, S. J. Self-Assembled, Chitosan  
1250 Grafted PLGA Nanoparticles for Intranasal Delivery: Design, Development and Ex Vivo Characterization.  
1251 *Polym Plast Technol Eng* **2013**, *52*, 368–380.
- 1252 110. Salade, L.; Wauthoz, N.; Deleu, M.; Vermeersch, M.; De Vriese, C.; Amighi, K.; Goole, J. Development of  
1253 coated liposomes loaded with ghrelin for nose-to-brain delivery for the treatment of cachexia. *Int J*  
1254 *Nanomedicine* **2017**, *12*, 8531–8543.
- 1255 111. Romana, B.; Batger, M.; Prestidge, C.; Colombo, G.; Sonvico, F. Expanding the Therapeutic Potential of  
1256 Statins by Means of Nanotechnology Enabled Drug Delivery Systems. *Curr Top Med Chem* **2014**, *14*, 1182–  
1257 1193.
- 1258 112. Sonvico, F.; Zimetti, F.; Pohlmann, A. R.; Guterres, S. S. Drug delivery to the brain: how can  
1259 nanoencapsulated statins be used in the clinic? *Ther Deliv* **2017**, *8*, 625–631.
- 1260 113. Clementino, A.; Batger, M.; Garrastazu, G.; Pozzoli, M.; Del Favero, E.; Rondelli, V.; Gutfilen, B.; Barboza,  
1261 T.; Sukkar, M. B.; Souza, S. A. L.; Cantù, L.; Sonvico, F. The nasal delivery of nanoencapsulated statins - an  
1262 approach for brain delivery. *Int J Nanomedicine* **2016**, *11*, 6575–6590.
- 1263 114. Kumar, M.; Misra, A.; Babbar, A. K.; Mishra, A. K.; Mishra, P.; Pathak, K. Intranasal nanoemulsion based  
1264 brain targeting drug delivery system of risperidone. *Int J Pharm* **2008**, *358*, 285–291.
- 1265 115. Samia, O.; Hanan, R.; Kamal, E. T. Carbamazepine mucoadhesive nanoemulgel (MNEG) as brain targeting  
1266 delivery system via the olfactory mucosa. *Drug Deliv* **2012**, *19*, 58–67.

- 1267 116. Perez, A. P.; Mundiña-Weilenmann, C.; Romero, E. L.; Morilla, M. J. Increased brain radioactivity by  
1268 intranasal P-labeled siRNA dendriplexes within in situ-forming mucoadhesive gels. *Int J Nanomedicine*  
1269 **2012**, *7*, 1373–1385.
- 1270 117. Jain, D. S.; Bajaj, A. N.; Athawale, R. B.; Shikhande, S. S.; Pandey, A.; Goel, P. N.; Gude, R. P.; Patil, S.;  
1271 Raut, P. Thermosensitive PLA based nanodispersion for targeting brain tumor via intranasal route. *Mater*  
1272 *Sci Eng C Mater Biol Appl* **2016**, *63*, 411–421.
- 1273 118. Wavikar, P. R.; Vavia, P. R. Rivastigmine-loaded in situ gelling nanostructured lipid carriers for nose to  
1274 brain delivery. *J Liposome Res* **2015**, *25*, 141–149.
- 1275 119. Hao, J.; Zhao, J.; Zhang, S.; Tong, T.; Zhuang, Q.; Jin, K.; Chen, W.; Tang, H. Fabrication of an ionic-  
1276 sensitive in situ gel loaded with resveratrol nanosuspensions intended for direct nose-to-brain delivery.  
1277 *Colloids Surf B Biointerfaces* **2016**, *147*, 376–386.
- 1278 120. Sigurdsson, H. H.; Kirch, J.; Lehr, C.-M. Mucus as a barrier to lipophilic drugs. *Int J Pharm* **2013**, *453*, 56–64.
- 1279 121. Lieleg, O.; Ribbeck, K. Biological hydrogels as selective diffusion barriers. *Trends in Cell Biology* **2011**, *21*,  
1280 543–551.
- 1281 122. Cone, R. A. Barrier properties of mucus. *Adv Drug Deliv Rev* **2009**, *61*, 75–85.
- 1282 123. Vila, A.; Gill, H.; McCallion, O.; Alonso, M. J. Transport of PLA-PEG particles across the nasal mucosa:  
1283 Effect of particle size and PEG coating density. *J Control Release* **2004**, *98*, 231–244.
- 1284 124. Schuster, B. S.; Suk, J. S.; Woodworth, G. F.; Hanes, J. Nanoparticle diffusion in respiratory mucus from  
1285 humans without lung disease. *Biomaterials* **2013**, *34*, 3439–3446.
- 1286 125. Lai, S. K.; Suk, J. S.; Pace, A.; Wang, Y.-Y.; Yang, M.; Mert, O.; Chen, J.; Kim, J.; Hanes, J. Drug carrier  
1287 nanoparticles that penetrate human chronic rhinosinusitis mucus. *Biomaterials* **2011**, *32*, 6285–6290.
- 1288 126. Mert, O.; Lai, S. K.; Ensign, L.; Yang, M.; Wang, Y.-Y.; Wood, J.; Hanes, J. NANOMEDICINE. *J Control*  
1289 *Release* **2012**, *157*, 455–460.
- 1290 127. Xu, Q.; Boylan, N. J.; Cai, S.; Miao, B.; Patel, H.; Hanes, J. Scalable method to produce biodegradable  
1291 nanoparticles that rapidly penetrate human mucus. *J Control Release* **2013**, *170*, 279–286.
- 1292 128. Kirch, J.; Schneider, A.; Abou, B.; Hopf, A.; Schaefer, U. F.; Schneider, M.; Schall, C.; Wagner, C.; Lehr, C.-  
1293 M. Optical tweezers reveal relationship between microstructure and nanoparticle penetration of  
1294 pulmonary mucus. *Proc Natl Acad Sci USA* **2012**, *109*, 18355–18360.
- 1295 129. Sharma, D.; Sharma, R. K.; Bhatnagar, A.; Nishad, D. K.; Singh, T.; Gabrani, R.; Sharma, S. K.; Ali, J.; Dang,  
1296 S. Nose to Brain Delivery of Midazolam Loaded PLGA Nanoparticles: In Vitro and In Vivo Investigations.  
1297 *Curr Drug Deliv* **2016**, *13*, 557–564.
- 1298 130. Sekerdag, E.; Lüle, S.; Bozdağ Pehlivan, S.; Öztürk, N.; Kara, A.; Kaffashi, A.; Vural, I.; Işıkkay, I.; Yavuz, B.;  
1299 Oguz, K. K.; Söylemezoğlu, F.; Gürsoy-Özdemir, Y.; Mut, M. A potential non-invasive glioblastoma  
1300 treatment: Nose-to-brain delivery of farnesylthiosalicylic acid incorporated hybrid nanoparticles. *J Control*  
1301 *Release* **2017**, *261*, 187–198.
- 1302 131. Zhang, Q.-Z.; Zha, L.-S.; Zhang, Y.; Jiang, W.-M.; Lu, W.; Shi, Z.-Q.; Jiang, X.-G.; Fu, S.-K. The brain  
1303 targeting efficiency following nasally applied MPEG-PLA nanoparticles in rats. *J Drug Target* **2006**, *14*, 281–  
1304 290.
- 1305 132. Wang, Y.-Y.; Lai, S. K.; Suk, J. S.; Pace, A.; Cone, R.; Hanes, J. Addressing the PEG mucoadhesivity  
1306 paradox to engineer nanoparticles that “slip” through the human mucus barrier. *Angew Chem Int Ed Engl*  
1307 **2008**, *47*, 9726–9729.

- 1308 133. Behrens, I.; Pena, A. I. V.; Alonso, M. J.; Kissel, T. Comparative uptake studies of bioadhesive and non-  
1309 bioadhesive nanoparticles in human intestinal cell lines and rats: the effect of mucus on particle adsorption  
1310 and transport. *Pharm Res* **2002**, *19*, 1185–1193.
- 1311 134. Salmaso, S.; Caliceti, P. Stealth properties to improve therapeutic efficacy of drug nanocarriers. *J Drug*  
1312 *Deliv* **2013**, *2013*, 374252.
- 1313 135. Guo, Y.; Luo, J.; Tan, S.; Otieno, B. O.; Zhang, Z. The applications of Vitamin E TPGS in drug delivery. *Eur*  
1314 *J Pharm Sci* **2013**, *49*, 175–186.
- 1315 136. Jain, R.; Nabar, S.; Dandekar, P.; Patravale, V. Micellar nanocarriers: potential nose-to-brain delivery of  
1316 zolmitriptan as novel migraine therapy. *Pharm Res* **2010**, *27*, 655–664.
- 1317 137. Jain, R.; Nabar, S.; Dandekar, P.; Hassan, P.; Aswal, V.; Talmon, Y.; Shet, T.; Borde, L.; Ray, K.; Patravale,  
1318 V. Formulation and evaluation of novel micellar nanocarrier for nasal delivery of sumatriptan.  
1319 *Nanomedicine (London, England)* **2010**, *5*, 575–587.
- 1320 138. Salama, H. A.; Mahmoud, A. A.; Kamel, A. O.; Abdel Hady, M.; Awad, G. A. S. Phospholipid based  
1321 colloidal poloxamer-nanocubic vesicles for brain targeting via the nasal route. *Colloids Surf B Biointerfaces*  
1322 **2012**, *100*, 146–154.
- 1323 139. Abdelrahman, F. E.; Elsayed, I.; Gad, M. K.; Elshafeey, A. H.; Mohamed, M. I. Response surface  
1324 optimization, Ex vivo and In vivo investigation of nasal spanlastics for bioavailability enhancement and  
1325 brain targeting of risperidone. *Int J Pharm* **2017**, *530*, 1–11.
- 1326 140. Zhao, Y.-Z.; Li, X.; Lu, C.-T.; Lin, M.; Chen, L.-J.; Xiang, Q.; Zhang, M.; Jin, R. R.; Jiang, X.; Shen, X.-T.; Li,  
1327 X.-K.; Cai, J. Gelatin nanostructured lipid carriers-mediated intranasal delivery of basic fibroblast growth  
1328 factor enhances functional recovery in hemiparkinsonian rats. *Nanomedicine* **2014**, *10*, 755–764.
- 1329 141. Bhatt, R.; Singh, D.; Prakash, A.; Mishra, N. Development, characterization and nasal delivery of  
1330 rosmarinic acid-loaded solid lipid nanoparticles for the effective management of Huntington's disease.  
1331 *Drug Deliv* **2015**, *22*, 931–939.
- 1332 142. Illum, L. Nasal drug delivery--possibilities, problems and solutions. *J Control Release* **2003**, *87*, 187–198.
- 1333 143. Abd-Elal, R. M. A.; Shamma, R. N.; Rashed, H. M.; Bendas, E. R. Trans-nasal zolmitriptan novasomes: in-  
1334 vitro preparation, optimization and in-vivo evaluation of brain targeting efficiency. *Drug Deliv* **2016**, *23*,  
1335 3374–3386.
- 1336 144. Singh, A. P.; Saraf, S. K.; Saraf, S. A. SLN approach for nose-to-brain delivery of alprazolam. *Drug Deliv*  
1337 *Transl Res* **2012**, *2*, 498–507.
- 1338 145. Mehra, N. K.; Mishra, V.; Jain, N. K. Receptor-based targeting of therapeutics. *Ther Deliv* **2013**, *4*, 369–394.
- 1339 146. Ruenaroengsak, P.; Cook, J. M.; Florence, A. T. Nanosystem drug targeting: Facing up to complex  
1340 realities. *J Control Release* **2010**, *141*, 265–276.
- 1341 147. Bies, C.; Lehr, C.-M.; Woodley, J. F. Lectin-mediated drug targeting: history and applications. *Adv Drug*  
1342 *Deliv Rev* **2004**, *56*, 425–435.
- 1343 148. Broadwell, R. D.; Balin, B. J. Endocytic and exocytic pathways of the neuronal secretory process and trans  
1344 synaptic transfer of wheat germ agglutinin-horseradish peroxidase in vivo. *J Comp Neurol* **1985**, *242*, 632–  
1345 650.
- 1346 149. Thorne, R. G.; Emory, C. R.; Ala, T. A.; Frey, W. H. Quantitative analysis of the olfactory pathway for drug  
1347 delivery to the brain. *Brain Res* **1995**, *692*, 278–282.
- 1348 150. Gao, X.; Tao, W.; Lu, W.; Zhang, Q.; Zhang, Y.; Jiang, X.; Fu, S. Lectin-conjugated PEG-PLA nanoparticles:  
1349 preparation and brain delivery after intranasal administration. *Biomaterials* **2006**, *27*, 3482–3490.

- 1350 151. Liu, Q.; Shen, Y.; Chen, J.; Gao, X.; Feng, C.; Wang, L.; Zhang, Q.; Jiang, X. Nose-to-brain transport  
1351 pathways of wheat germ agglutinin conjugated PEG-PLA nanoparticles. *Pharm Res* **2012**, *29*, 546–558.
- 1352 152. Gao, X.; Wu, B.; Zhang, Q.; Chen, J.; Zhu, J.; Zhang, W.; Rong, Z.; Chen, H.; Jiang, X. Brain delivery of  
1353 vasoactive intestinal peptide enhanced with the nanoparticles conjugated with wheat germ agglutinin  
1354 following intranasal administration. *J Control Release* **2007**, *121*, 156–167.
- 1355 153. Gao, X.; Chen, J.; Chen, J.; Wu, B.; Chen, H.; Jiang, X. Quantum Dots Bearing Lectin-Functionalized  
1356 Nanoparticles as a Platform for In Vivo Brain Imaging. *Bioconjug Chem* **2008**, *19*, 2189–2195.
- 1357 154. Chen, J.; Zhang, C.; Liu, Q.; Shao, X.; Feng, C.; Shen, Y.; Zhang, Q.; Jiang, X. Solanum tuberosumlectin-  
1358 conjugated PLGA nanoparticles for nose-to-brain delivery: in vivo and in vitro evaluations. *J Drug Target*  
1359 **2011**, *20*, 174–184.
- 1360 155. Gao, X.; Chen, J.; TAO, W.; Zhu, J.; ZHANG, Q.; CHEN, H.; Jiang, X. UEA I-bearing nanoparticles for  
1361 brain delivery following intranasal administration. *Int J Pharm* **2007**, *340*, 207–215.
- 1362 156. Wen, Z.; Yan, Z.; He, R.; Pang, Z.; Guo, L.; Qian, Y.; Jiang, X.; Fang, L. Brain targeting and toxicity study of  
1363 odorranalectin-conjugated nanoparticles following intranasal administration. *Drug Deliv* **2011**, *18*, 555–561.
- 1364 157. Piazza, J.; Hoare, T.; Molinaro, L.; Terpstra, K.; Bhandari, J.; Selvaganapathy, P. R.; Gupta, B.; Mishra, R. K.  
1365 Haloperidol-loaded intranasally administered lectin functionalized poly(ethylene glycol)-block-poly(d,l)-  
1366 lactic-co-glycolic acid (PEG-PLGA) nanoparticles for the treatment of schizophrenia. *Eur J Pharm Biopharm*  
1367 **2014**, *87*, 30–39.
- 1368 158. Wen, Z.; Yan, Z.; Hu, K.; Pang, Z.; Cheng, X.; Guo, L.; Zhang, Q.; Jiang, X.; Fang, L.; Lai, R. Odorranalectin-  
1369 conjugated nanoparticles: Preparation, brain delivery and pharmacodynamic study on Parkinson's disease  
1370 following intranasal administration. *J Control Release* **2011**, *151*, 131–138.
- 1371 159. Liu, Q.; Shao, X.; Chen, J.; Shen, Y.; Feng, C.; Gao, X.; Zhao, Y.; Li, J.; Zhang, Q.; Jiang, X. In vivo toxicity  
1372 and immunogenicity of wheat germ agglutinin conjugated poly(ethylene glycol)-poly(lactic acid)  
1373 nanoparticles for intranasal delivery to the brain. *Toxicol Appl Pharmacol* **2011**, *251*, 79–84.
- 1374 160. Fonseca, S. B.; Pereira, M. P.; Kelley, S. O. Recent advances in the use of cell-penetrating peptides for  
1375 medical and biological applications. *Adv Drug Deliv Rev* **2009**, *61*, 953–964.
- 1376 161. Lin, T.; Liu, E.; He, H.; Shin, M. C.; Moon, C.; Yang, V. C.; Huang, Y. Nose-to-brain delivery of  
1377 macromolecules mediated by cell-penetrating peptides. *Acta Pharm Sin B* **2016**, *6*, 352–358.
- 1378 162. Xia, H.; Gao, X.; Gu, G.; Liu, Z.; Zeng, N.; Hu, Q.; Song, Q.; Yao, L.; Pang, Z.; Jiang, X.; Chen, J.; Chen, H.  
1379 Low molecular weight protamine-functionalized nanoparticles for drug delivery to the brain after  
1380 intranasal administration. *Biomaterials* **2011**, *32*, 9888–9898.
- 1381 163. Kanazawa, T.; Taki, H.; Tanaka, K.; Takashima, Y.; Okada, H. Cell-penetrating peptide-modified block  
1382 copolymer micelles promote direct brain delivery via intranasal administration. *Pharm Res* **2011**, *28*, 2130–  
1383 2139.
- 1384 164. Taki, H.; Kanazawa, T.; Akiyama, F.; Takashima, Y.; Okada, H. Intranasal Delivery of Camptothecin-  
1385 Loaded Tat-Modified Nanomicelles for Treatment of Intracranial Brain Tumors. *Pharmaceutics* **2012**, *5*,  
1386 1092–1102.
- 1387 165. Kanazawa, T.; Akiyama, F.; Kakizaki, S.; Takashima, Y.; Seta, Y. Delivery of siRNA to the brain using a  
1388 combination of nose-to-brain delivery and cell-penetrating peptide-modified nano-micelles. *Biomaterials*  
1389 **2013**, *34*, 9220–9226.
- 1390 166. Rassa, G.; Soddu, E.; Posadino, A. M.; Pintus, G.; Sarmiento, B.; Giunchedi, P.; Gavini, E. Nose-to-brain  
1391 delivery of BACE1 siRNA loaded in solid lipid nanoparticles for Alzheimer's therapy. *Colloids Surf B*  
1392 *Biointerfaces* **2017**, *152*, 296–301.

- 1393 167. Frenkel, D.; Solomon, B. Filamentous phage as vector-mediated antibody delivery to the brain. *Proc Natl*  
1394 *Acad Sci USA* **2002**, *99*, 5675–5679.
- 1395 168. Janda, K. J. Delivery of Active Proteins to the Central Nervous System Using Phage Vectors, European  
1396 Patent Office **2008**, EP1898701 A1.
- 1397 169. Suzuki, Y. A.; Lopez, V.; Lönnnerdal, B. Mammalian lactoferrin receptors: Structure and function. *Cell Mol*  
1398 *Life Sci* **2005**, *62*, 2560–2575.
- 1399 170. Elfinger, M.; Maucksch, C.; Rudolph, C. Characterization of lactoferrin as a targeting ligand for nonviral  
1400 gene delivery to airway epithelial cells. *Biomaterials* **2007**, *28*, 3448–3455.
- 1401 171. Liu, Z.; Jiang, M.; Kang, T.; Miao, D.; Gu, G.; Song, Q.; Yao, L.; Hu, Q.; Tu, Y.; Pang, Z.; Chen, H.; Jiang, X.;  
1402 Gao, X.; Chen, J. Lactoferrin-modified PEG-co-PCL nanoparticles for enhanced brain delivery of NAP  
1403 peptide following intranasal administration. *Biomaterials* **2013**, *34*, 3870–3881.
- 1404 172. Bi, C. C.; Wang, A. P.; Chu, Y. C.; Liu, S.; Mu, H. J.; Liu, W. H.; Wu, Z. M.; Sun, K. X.; Li, Y. X. Intranasal  
1405 delivery of rotigotine to the brain with lactoferrin-modified PEG-PLGA nanoparticles for Parkinson's  
1406 disease treatment. *Int J Nanomedicine* **2016**, *11*, 6547–6559.
- 1407 173. Pan, L.; Zhou, J.; Ju, F.; Zhu, H. Intranasal delivery of  $\alpha$ -asarone to the brain with lactoferrin-modified  
1408 mPEG-PLA nanoparticles prepared by premix membrane emulsification. *Drug Deliv Transl Res* **2018**, *8*, 83–  
1409 96.
- 1410 174. Liu, L.; Zhang, X.; Li, W.; Sun, H.; Lou, Y.; Zhang, X.; Li, F. Transferrin receptor antibody-modified  $\alpha$ -  
1411 cobrotoxin-loaded nanoparticles enable drug delivery across the blood–brain barrier by intranasal  
1412 administration. *J Nanopart Res* **2013**, *15*, 2059.
- 1413 175. Hoekman, J. D.; Srivastava, P.; Ho, R. J. Y. Aerosol-stable peptide-coated liposome nanoparticles: a proof-  
1414 of-concept study with opioid fentanyl in enhancing analgesic effects and reducing plasma drug exposure. *J*  
1415 *Pharm Sci* **2014**, *103*, 2231–2239.